

 Open access • Posted Content • DOI:10.1101/2020.11.02.365247

Shared genetic architecture underlying root metaxylem phenotypes under drought stress in cereals — Source link

Stephanie P. Klein, Jenna E. Reeger, Shawn M. Kaeppler, Kathleen M. Brown ...+1 more authors

Institutions: Pennsylvania State University, University of Wisconsin-Madison

Published on: 02 Nov 2020 - bioRxiv (Cold Spring Harbor Laboratory)

Topics: Candidate gene

Related papers:

- [Identification of gene modules associated with drought response in rice by network-based analysis.](#)
- [Genetic control of root plasticity in response to salt stress in maize](#)
- [Functional mechanisms of drought tolerance in subtropical maize \(*Zea mays* L.\) identified using genome-wide association mapping.](#)
- [Comparative alternative splicing analysis of two contrasting rice cultivars under drought stress and association of differential splicing genes with drought response QTLs](#)
- [The transcriptomic landscapes of rice cultivars with diverse root system architectures grown in upland field conditions.](#)

Share this paper:    

View more about this paper here: <https://typeset.io/papers/shared-genetic-architecture-underlying-root-metaxylem-1qd86fz5i2>

1 Short title: Maize and rice root metaxylem GWAS

2 Corresponding author: Jonathan P. Lynch, jpl4@psu.edu, 814-863-2256

3 Article title: Shared genetic architecture underlying root metaxylem phenotypes under drought
4 stress in cereals

5 Authors: Stephanie P. Klein¹, Jenna E. Reeger¹, Shawn M. Kaeppler², Kathleen M. Brown¹,
6 Jonathan P. Lynch¹

7 ¹Department of Plant Science, The Pennsylvania State University, University Park, PA 16802,
8 USA; ²Department of Agronomy, University of Wisconsin, Madison, WI 53706, USA

9 spk185@psu.edu

10 jer302@psu.edu

11 smkaeapl@wisc.edu

12 kbe@psu.edu

13 One sentence summary: Cross-species genome-wide association studies and a gene co-
14 expression network identified genes associated with root metaxylem phenotypes in maize under
15 water stress and non-stress and rice.

16 Author contributions: SPK designed the experiments, analyzed the data, and wrote the article
17 with contributions from all authors; JER analyzed data and contributed to writing; SMK and
18 KMB provided feedback on data analysis and writing; JPL conceived and supervised the project
19 and contributed to data analysis and writing. JPL agrees to serve as the author responsible for
20 contact and ensures communication.

21 Date of submission:

22 Number of Tables: 3

23 Number of Figures: 6

24 Abstract Length: 197

25 Word Count: 8594

26 **Abstract**

27 Root metaxylem are phenotypically diverse structures whose function is related to their anatomy,
28 particularly under drought stress. Much research has dissected the genetic machinery underlying
29 metaxylem phenotypes in dicots, but monocots are relatively unexplored. In maize (*Zea mays*), a
30 robust pipeline integrated a GWAS of root metaxylem phenes under well-watered and water
31 stress conditions with a gene co-expression network to identify candidate genes most likely to
32 impact metaxylem phenotypes. We identified several promising candidate genes in 14 gene co-
33 expression modules inferred to be functionally relevant to xylem development. We also
34 identified five gene candidates that co-localized in multiple root metaxylem phenes in both well-
35 watered and water stress conditions. Using a rice GWAS conducted in parallel, we detected
36 overlapping genetic architecture influencing root metaxylem phenotypes by identifying eight
37 pairs of syntenic candidate genes significantly associated with metaxylem phenes. There is
38 evidence that the genes of these syntenic pairs may be involved in biosynthetic processes related
39 to the cell wall, hormone signaling, oxidative stress responses, and drought responses. Our study
40 demonstrates a powerful new strategy for identifying promising gene candidates and suggests
41 several gene candidates that may enhance our understanding of vascular development and
42 responses to drought in cereals.

43 **Abbreviations:**

44 ABA: abscisic acid

45 BN: bottleneck gene

46 BN/HUB: bottleneck and hub gene

47 GWAS: genome-wide association study

48 HUB: hub gene

49 SNP: single nucleotide polymorphism

50 WS: water stress

51 WW: well-watered

52 **Introduction**

53 Drought is a primary constraint to crop production worldwide and its effects are only predicted
54 to worsen in the coming decades as a result of climate change (Lobell et al., 2011; Dai, 2013;
55 IPCC, 2013). Plant breeding efforts have been aimed at maintaining crop productivity in stressful
56 environments in order to sustain growing agriculture-centric economies and to meet increasing
57 consumer demand. As the primary organ responsible for the sensing and uptake of water, roots
58 have become a focus for crop improvement under drought (Lynch et al., 2014; Vadez, 2014).
59 Recent efforts have sought to approach root-focused breeding by selecting for a root system
60 architecture better adapted to water-limited conditions (Ho et al., 2005; Lynch, 2013; Li et al.,
61 2018; Zhang et al., 2019; BurrIDGE et al., 2020). For instance, a steep root growth angle that
62 increases rooting depth has been associated with improved tolerance to water scarcity in maize
63 (Liakat Ali et al., 2015; Pires et al., 2020) and rice (Uga et al., 2013). Fewer nodal roots with
64 more sparsely distributed long lateral roots is also associated with improved drought tolerance
65 (Zhan et al., 2015; Gao and Lynch, 2016; Lynch, 2019). Several anatomical phenes have been
66 proposed to mitigate drought effects by facilitating the capture of mobile resources, such as
67 water and nitrogen, deep in the soil profile (Lynch, 2013; Lynch et al., 2014; Lynch, 2018;
68 Lynch, 2019). Increased aerenchyma production (Zhu et al., 2010; Jaramillo et al., 2013) and
69 larger cortical cells arranged in fewer files cheapen the root maintenance costs (Chimungu et al.,
70 2014a; Chimungu et al., 2014b), which would allow more resources to be reallocated to deeper
71 root construction (Lynch, 2013; Lynch et al., 2014). Additionally, many architectural and
72 anatomical phenes are plastic, which may be an adaptive response to drought stress (Kano et al.,
73 2011; Klein et al., 2020; Schneider et al., 2020a; Schneider and Lynch, 2020; Schneider et al.,
74 2020b). However, less attention has been paid to root hydraulics, which have direct implications
75 for water uptake and transport (Wasson et al., 2012; Vadez, 2014; Maurel and Nacry, 2020).

76 Maize, one of the world's most economically and nutritionally important crops, is particularly
77 sensitive to drought stress (Lobell et al., 2014; Daryanto et al., 2016). Root metaxylem vessels
78 are a natural target to improve maize since their size and number in the root is related to abiotic
79 stress tolerance (Richards and Passioura, 1989; Comas et al., 2013). Several studies have found
80 an association between drought tolerance and metaxylem vessel number (de Souza et al., 2013;
81 Klein et al., 2020) or metaxylem vessel area (Richards and Passioura, 1989; Abd Allah et al.,

82 2010; Purushothaman et al., 2013; de Souza et al., 2013; Klein et al., 2020). Plants with narrower
83 root metaxylem have reduced hydraulic conductivity but more conservative water usage and
84 greater resistance to cavitation (Richards and Passioura, 1989; Sperry and Saliendra, 1994;
85 Vilagrosa et al., 2012; Guet et al., 2015). Given that hydraulic conductance is proportional to the
86 vessel radius raised to the fourth power according to the Hagen-Poiseuille equation, even a slight
87 narrowing of the metaxylem vessels will result in a considerable reduction in axial conductivity.
88 Conservative water usage as a result of restricted hydraulic conductance, especially early in the
89 growing season, has been suggested to be more effective than deeper rooting by making water
90 access more likely during the critical anthesis-silking interval (Zaman-Allah et al., 2011; Feng et
91 al., 2016). Reduced transpiration due to restricted hydraulic conductance from narrow
92 metaxylem vessels may also be beneficial for mitigating drought effects by inducing stomatal
93 closure, increasing water use efficiency by reducing the overall shoot size, and retaining
94 moisture at the root tips to enable further growth through the soil profile (Vadez et al., 2014;
95 Lynch, 2019). A constitutive reduction in metaxylem vessel area could limit plant maximum
96 potential growth or reduce relative growth rates (λ) under well-watered conditions (Wahl and
97 Ryser, 2000; Comas et al., 2013), but these effects may be counteracted by augmenting the
98 number of metaxylem vessels (Lynch et al., 2014). Metaxylem phenes that improve performance
99 under water stress with no penalty under optimal conditions are of utmost importance to identify.

100 Metaxylem vessels form through the careful coordination of phytohormone biosynthesis and
101 signaling, cell wall formation and lignification, cell expansion, radial patterning, and
102 programmed cell death (Roberts and McCann, 2000; Schuetz et al., 2012; Milhinhos and Miguel,
103 2013; Růžička et al., 2015). Decades of research have deepened our understanding of the genetic
104 and developmental underpinnings of xylem development but has mostly been limited to
105 dicotyledonous or woody species. Recent studies have identified two quantitative trait loci
106 intervals associated with xylem area traits in spring barley (*Hordeum vulgare*) (Oyiga et al.,
107 2020) and a few genetic loci associated with root metaxylem size and number in rice (*Oryza*
108 *sativa*) (Kadam et al., 2017). However, the genetic mechanisms regulating xylem development in
109 grain crops is still poorly understood. Arranged in a polyarchy pattern (Hochholdinger, 2009),
110 the vascular organization of monocot roots, such as members of the *Poaceae*, is structurally
111 distinct from di-, tri-, or tetrarch patterns typical of most dicots. Cell wall composition also
112 differs between dicots and monocots, since monocots are richer in hydroxycinnamates and

113 hemicellulose with little pectin or structural protein content (Carpita, 1996; Smith and Harris,
114 1999; Vogel, 2008). Despite these differences, shared genetic machinery underlying xylem
115 development is likely, as is the case for example for the cellulose synthase A (CesA) gene
116 family, which is present in all seed plants (Richmond and Somerville, 2000). Furthermore,
117 comparisons between maize and closely related species have found shared genetic architecture
118 influencing sorghum (*Sorghum bicolor*) root architecture (Zheng et al., 2020) and rice (*Oryza*
119 *sativa*) grain development (Chen et al., 2016). These studies suggest there is a high likelihood
120 that the genetic machinery regulating other developmental processes, like xylem development,
121 may be conserved within monocots.

122 Plasticity in xylem phenotypes in response to drought has been observed in maize (Klein et al.,
123 2020; Schneider et al., 2020a), rice (Henry et al., 2012; Kadam et al., 2017), and wheat (*Triticum*
124 *aestivum*) (Kadam et al., 2015), and are likely mediated by stress-responsive cellular and genetic
125 factors. The genetic mechanisms underlying drought-induced variation in root xylem phenotypes
126 are largely unknown. Several genes regulating biosynthesis and signaling of brassinosteroid,
127 cytokinin, ethylene, and gibberellin have been directly implicated in constitutive and abiotic
128 stress-responsive xylem development in dicot roots (Milhinhos and Miguel, 2013;
129 Ramachandran et al., 2020). However, these complex signaling cascades facilitated by hormones
130 are likely modified by crosstalk with other phytohormones like abscisic acid (ABA), whose
131 production increases in response to drought (Finkelstein, 2013; Ramachandran et al., 2020). In
132 maize, increased ABA production induced by drought coincides with increased root hydraulic
133 conductivity, which is likely mediated by augmented activity of root aquaporins rather than
134 changes to root metaxylem anatomy (Hose et al., 2000; Parent et al., 2009). More recent work
135 showed that ABA interfered with signaling among key developmental regulators and
136 subsequently altered root xylem phenotypes in *Arabidopsis* under limited water availability
137 (Ramachandran et al., 2018). However, there are likely many more genetic components
138 participating in these signaling cascades that contribute to variation in xylem phenotypes and
139 water uptake.

140 Novel breeding and phenotyping technologies have increased the capacity to evaluate and map
141 desirable characteristics to genetic loci in large populations, as is done in a genome-wide
142 association study (GWAS). Even so, many challenges remain when analyzing GWAS outputs to

143 avoid false positives and isolate the true loci with significant causal effects on phenotype. One
144 method to increase robustness of an associative mapping study is by conducting a comparative
145 multispecies GWAS, which has the potential to enhance our understanding of shared genetic
146 architectures among species (Chen et al., 2016; Zheng et al., 2020). Although maize and rice are
147 different in many respects (e.g. photosynthesis processes, tillering, etc.), their genomes share a
148 high degree of synteny (Bennetzen and Freeling, 1997; Salse et al., 2004; Buell et al., 2005), and
149 in the particular case of xylem phenes, both species have polyarch vascular arrangements.
150 Performing such a comparative GWAS between two grass species of high synteny, like maize
151 and rice, may reveal genetic architectures conserved among the cereals.

152 A second method to increase the robustness of GWAS is coupling it with a gene co-expression
153 network, which is a helpful tool to infer a candidate gene's biological function relative to the
154 functional role filled by comparably expressed genes (Schaefer et al., 2017; Schaefer et al.,
155 2018). Complex quantitative traits are often pleiotropic and are associated with many significant
156 SNPs with small effect sizes (Ingvarsson and Street, 2011). A candidate gene's topological
157 characteristics within the gene network may provide insight on its biological role and
158 essentiality. For instance, hub genes (genes that interact with a large number of other members
159 of the subnetwork) and bottleneck genes (genes with a high level of betweenness centrality) are
160 posited to be the most essential for proper function (Jeong et al., 2001; Yu et al., 2004; Yu et al.,
161 2007). Modifying or removing the activity of hub and bottleneck genes has the greatest chance of
162 inducing measurable downstream effects. Thus, integrating a GWAS with a gene co-expression
163 network is a powerful method to identify candidate genes with the highest likelihood of shaping
164 a measurable effect on phenotype and function.

165 Root metaxylem phenotypes merit greater attention because of their potential to improve crop
166 performance under water-limited conditions. One course of action is to dissect their genetic
167 architecture to provide insight on the loci and overarching mechanisms contributing to root
168 metaxylem phenotypic variation under abiotic stress. In this study, we phenotyped the root
169 metaxylem of a large diversity panel of field-grown maize under well-watered and water stress
170 conditions. A parallel study phenotyped the root metaxylem of a rice diversity panel grown in the
171 greenhouse under well-watered conditions (Vejchasarn 2014). Our objectives were to test the
172 hypotheses that 1.) natural variation in root metaxylem phenotypes is under genetic control; 2.)

173 genetic loci associated with root metaxylem phenotypes under WS are unique from those
174 activated under WW; and 3.) there is shared genetic architecture associated with root metaxylem
175 phenotypes in maize and rice.

176 **Results**

177 *Natural variation in root metaxylem phenotypes in the field*

178 Wide variation in all root metaxylem phenes was observed under both well-watered and water
179 deficit stress (hereafter, water stress) conditions in 180 and 412 genotypes of the Wisconsin
180 Diversity Panel in 2015 and 2016, respectively (Figure 1). A 3-4-fold range in values were
181 observed for all metaxylem phenes under both water treatments except for volumetric flow rate,
182 which exhibited a 31-fold range. Watering regime had no significant overall effect on metaxylem
183 phenotypes except for volumetric flow rate ($p = 0.036$) (Table 1), but responses to drought varied
184 by genotype (Supplemental Figure S1). Plasticity in all metaxylem vessel phenes in response to
185 water stress ranged from -84%-351% relative to the phene state in well-watered conditions.
186 While total metaxylem vessel area was stable between seasons, there were significant seasonal
187 effects for maximum and median metaxylem vessel areas, metaxylem vessel number, and
188 volumetric flow rate (Table 1). Volumetric flow rate was the only phene to exhibit a significant
189 interactive year and treatment effect.

190 Broad-sense and marker-based heritability on an entry mean basis was calculated within a shared
191 set of 95 genotypes. Broad-sense heritability ranged from 0.625 to 0.805 and marker-based
192 heritability ranged from 0.133-0.361, overall (Table 1). Repeatability was also calculated for the
193 collection of genotypes grown in each season and ranged from 0.602-0.827 in 2015 and 0.466-
194 0.670 in 2016 (Table 1).

195 *GWAS for metaxylem phenes*

196 A panel of 899,794 SNPs (Mazaheri et al., 2019) was used for GWAS on all root metaxylem
197 phenes under well-watered and water-stress conditions conducted with GAPIT (Lipka et al.,
198 2012). The fit of the model was corroborated with quantile-quantile (Q-Q) plots (Supplemental
199 Figure S2). Separate GWAS analyses were performed for each treatment and season of field
200 phenotype data to identify genetic loci that consistently exhibited similar effects on variance in
201 root metaxylem phenotypes. Despite differences in taxa membership in each season, there were

202 550,617 SNPs included in analyses of each season that were used to evaluate the consistency of
203 minor allele effects on phenotypes (Supplemental Figure S3A). Few of the SNPs omitted from
204 the comparison were significant in any analysis. Because of its larger genotype collection, the
205 2016 GWAS was designated the “testing set” to identify many genetic loci potentially associated
206 with root metaxylem phenotypes. The 2015 GWAS was the “validation set” to corroborate allelic
207 effects observed in the testing set. For the testing and validation sets, the allelic effect of each
208 SNP in each phene was converted to a percentile rank where 0 denoted a strong negative effect
209 and 100 indicated a strong positive effect on phenotype. A SNP with consistent allelic effects for
210 the same phene was one where the percentile rank in the validation set was within 10 percentile
211 points of its rank in the testing set (Supplemental Figure S3). This analysis was repeated for each
212 root metaxylem phene and treatment. The number of SNPs that displayed consistent allelic
213 effects was 24-28% of the full SNP panel included in each GWAS and varied among phenes and
214 treatments (Supplemental Table S2). A SNP was significant if it exceeded the p-threshold and
215 displayed consistent allelic effects on metaxylem phenotypes. No significant associations were
216 detected above the Bonferroni threshold of $-\log(p) = 9.08$. Thus, a more liberal threshold of
217 $-\log(p) = 3.43$ was applied to accommodate SNPs associated with small effect sizes (Figure 2).
218 This threshold was estimated using a model that took into account the average marker-based
219 heritability of all root metaxylem phenes and linkage disequilibrium in maize (Kaley and Purcell
220 2019).

221 Overall, 244 gene models contained or were within 5kb of 351 significant SNPs associated with
222 maize root metaxylem phenes under well-watered and water stress conditions (Table 2, Figure 2,
223 Supplemental Table S3). Under well-watered conditions, 181 significant SNPs located in or near
224 124 gene models were associated with metaxylem phenes (Table 2, Supplemental Table S3).
225 Under water stress, 176 significant SNPs located in or near 126 gene models were associated
226 with metaxylem phenes (Table 2, Supplemental Table S3). Several genomic regions displayed a
227 high density of significant SNPs associated with a specific phene (Figure 2). For instance, 13
228 gene models near 25 significant SNPs associated with total metaxylem vessel area under water
229 stress were detected in a region on chromosome 5. Another region on chromosome 3 contained 5
230 significant SNPs nearby two candidate gene models also associated with total metaxylem vessel
231 area under WS. Two gene models nearby 14 significant SNPs associated with median metaxylem
232 vessel area under water stress were detected on chromosome 2. Seven gene models near 12

233 significant SNPs associated with maximum and/or median metaxylem vessel area under well-
234 watered conditions were detected in a region on chromosome 6. Of the candidate genes
235 associated with root metaxylem phenes under well-watered and water stress, approximately 68%
236 were annotated for Mapman ontogenic categories (Supplemental Figure S4). However, there
237 were few differences in representation of Mapman ontogenic categories for candidate genes
238 associated with the well-watered treatment compared to those associated with water stress. A
239 slightly larger proportion of candidate genes identified under water stress were associated with
240 developmental processes while a larger proportion of candidate genes identified under well-
241 watered conditions were associated with stress responses.

242 The Variant Effect Predictor tool was used to assess the likelihood of the significant SNPs being
243 the causal SNP for mutation in the gene model (McLaren et al., 2016). In well-watered
244 conditions and water stress, approximately 35% and 22% of variants, respectively, generated
245 missense or 5' UTR variants, which are likely to affect protein function or transcriptional
246 regulation (Figure 3). Significant SNPs resulting in missense mutations were over three times as
247 prevalent in candidate genes associated with well-watered conditions (26.7% of all variants)
248 compared to water stress (7.7% of all variants). In both watering regimes, approximately 17% of
249 the SNPs resulted in synonymous mutations likely having no effect on protein function.
250 Nonsense mutations resulting in a premature stop codon were extremely rare.

251 We found 13 significant SNPs associated with six candidate genes co-localized in both watering
252 regimes (Figure 2, Supplemental Table S4). Several of these candidate genes also co-localized in
253 more than one metaxylem phene either by association with a single co-localized SNP or because
254 multiple SNPs residing near the gene were detected. Of these candidate genes, only one was
255 annotated. This gene was Zm00001d018394, DNA-binding protein phosphatase 2C (DBPTF2),
256 and contained four SNPs significantly associated with median root metaxylem vessel area in
257 both water treatments. The other five genes are not annotated, but their functional annotation
258 may be inferred according to its homology with genes characterized in *Arabidopsis* (Figure 2,
259 Supplemental Table S4). The gene Zm00001d028486 encodes a chemocyanin and contains two
260 SNPs associated with median and maximum root metaxylem vessel areas in both treatments and
261 volumetric flow rate under water stress. Zm00001d031332 encodes a heat shock protein and
262 contains four SNPs associated with median and maximum root metaxylem vessel areas under

263 well-watered and water stress conditions. Two SNPs nearby Zm00001d038573, a ubiquitin
264 domain containing 1, and Zm00001d038754, an endoplasmic reticulum lumen protein retaining
265 receptor, were associated with maximum and median root metaxylem vessel area in both
266 treatments. Finally, the gene Zm00001d045954 encodes a RNA binding protein that contains one
267 SNP significantly associated with maximum root metaxylem vessel area in both treatments.

268 *Gene Co-expression Network of root tissues*

269 To identify groups of genes with a high likelihood of regulating root xylem phenotypes, the
270 WGCNA package (Langfelder and Horvath, 2008) was used to discover gene co-expression
271 relationship networks among expressed genes in 19 root tissues (Stelpflug et al., 2016) (Figure
272 4). Using a signed network analysis, 39 modules of co-expressed genes were identified, each one
273 labeled as a color (Figure 4A). The membership of each module ranged from 35
274 (“lavenderblush3”) to 5070 (“black”) genes. Of those, 14 modules had greater potential for being
275 associated with metaxylem phenotypes because of the significant correlation between the module
276 eigengene and root tissue samples relevant to xylem development (Figure 4B). Root tissues most
277 relevant to xylem development ($-\log(p) > 2$) are the stele 3 days after sowing (DAS) (modules
278 “lightcyan”, “thistle2”, “yellowgreen”), the differentiation zone 3 DAS (“darkred”, “lightcyan1”,
279 “red”), the meristematic and elongation zone 3 DAS (“black”, “lightgreen”, “thistle1”), the
280 whole root system 3 DAS (“salmon4”), zone 1 of the primary root 7 DAS (“mediumpurple3”,
281 “orange”), and zone 2 of the primary root 7 DAS (“darkgreen”, “navajowhite2”). Gene ontology
282 (GO) analysis showed that several biological functions related to xylem development were over-
283 represented in the xylem-related modules (Figure 4C). Modules “black” and “lightgreen” were
284 most strongly associated with root morphology and anatomical development whereas module
285 “thistle2” was particularly associated with the cell wall and carbohydrate biosynthesis. GO terms
286 related to signaling were most strongly represented in modules “lightcyan”, “lightgreen” and
287 “yellowgreen”. While the “black” module was most strongly associated with stress responses,
288 six additional modules were shown to be associated with stress responses as well. No GO terms
289 were over-represented by modules “lightcyan1”, “thistle1” and “salmon4” (not shown).

290 Of the 244 significant gene candidates identified in the GWAS, 103 reside in gene co-expression
291 modules relevant to xylem development – 57 under well-watered conditions and 50 under water
292 stress (Table 2). Topology metrics of each module’s network were used to infer the essentiality

293 of each gene within the network (Supplemental Table S5). Hub genes (HUB), or those that were
294 most connected to the rest of the network, exhibit a high closeness centrality while bottleneck
295 genes (BN), those through which many connections are channeled, exhibit a high betweenness
296 centrality. A gene may be both a bottleneck and hub (BN/HUB). Within the network of each co-
297 expression module, genes in the 80th percentile and above of closeness centrality and
298 betweenness centrality were classified as hub and bottleneck genes, respectively (Supplemental
299 Figures S5). Of the GWAS candidate genes that reside in stele-related modules (“lightcyan”,
300 “thistle2”, “yellowgreen”), 3 hub genes, 1 bottleneck genes, and 3 bottleneck/hub genes were
301 identified (Figure 5). Only one of these genes is annotated: ferritin homolog2 (FER2;
302 Zm00001d023225), a hypothetical bottleneck/hub gene from “thistle2” associated with root
303 metaxylem vessel number under well-watered conditions (Figure 5)..

304 Comparative GWAS on metaxylem phenes between maize and rice

305 Because the development of metaxylem phenotypes in maize and rice is similar, we
306 hypothesized that these species have shared genetic control for metaxylem phenotypes. To test
307 this hypothesis, we compared the unique candidate genes from each maize and rice GWAS to
308 identify syntenic genes that were similarly significant in each analysis. We identified eight pairs
309 of syntenic genes in maize and rice that were significantly associated with metaxylem phenes in
310 a GWAS: six were related to maize grown under well-watered conditions and two were related
311 to maize grown under water stress (Figure 6A, Table 3). Five of these syntenic pairs were
312 similarly associated with size-related metaxylem phenes (maximum, median and total
313 metaxylem vessel areas; volumetric flow rate) or vessel number in both maize and rice. Some of
314 these genes may share similar functional roles since several metabolic pathways were
315 represented by at least two syntenic pairs. Two maize genes (Zm00001d008569,
316 Zm00001d046838) and their respective rice homologs (Os01g0134500, Os06g0334300) are
317 active in the brassinosteroid biosynthesis pathway and were each associated with metaxylem
318 size-related phenes under well-watered conditions (Table 3). Four of these syntenic gene pairs
319 are associated with drought responses. Zm00001d038999 encodes the maize protein drought-
320 induced 19 and was associated with maximum and median vessel area in maize under well-
321 watered conditions, while its rice homolog (Os05g0562200) was associated with metaxylem
322 vessel number in the *indica* rice subpopulation. Zm00001d048165 and its rice homolog

323 Os03g0353400 encode the protein EARLY RESPONSIVE TO DEHYDRATION 15, which was
324 similarly associated with metaxylem vessel number in the full rice population and maize under
325 WS. However, there were no significant associations between the minor allele and root
326 metaxylem phenotypes observed in maize or rice for either of these genes.

327 A root-specific kinase 1, Zm00001d014243 and its rice homolog Os10g0395000, were similarly
328 associated with metaxylem size-related phenes under well-watered conditions: volumetric flow
329 rate in maize and median root metaxylem vessel area in the *aus* rice subpopulation (Figure 6). In
330 maize, individuals containing the minor allele exhibited on average a significantly lower
331 volumetric flow rate compared to the rest of the population ($p < 0.001$; Figure 6). Substitution
332 with this minor allele results in a missense mutation leading to a replacement of serine for
333 threonine. Because it was distant from the associated significant SNP in rice, phenotypic
334 differences were evaluated for various haplotypes of the gene candidate (Supplemental Figure
335 S6). There were significant differences ($p < 0.001$) in root metaxylem vessel area among
336 haplotypes where individuals with haplotype 4 contained the smallest root metaxylem vessel area
337 and those of haplotype 7 contained the largest (Figure 6). BLAST was used to collect highly
338 similar sequences of this gene in other species. This syntenic gene pair exhibited a high degree of
339 homology with root specific kinases and serine/threonine protein kinases of several other
340 monocotyledonous species (Figure 6). Root-specific kinase 1 also has several homologs in maize
341 and rice. No sequences of dicots were identified under these parameters.

342

343 **Discussion**

344 Since metaxylem anatomy has important implications for hydraulic function (Hacke and Sperry,
345 2001; Comas et al., 2013), the genetic architecture of root metaxylem phenotypes has important
346 implications for plant performance under drought. We identified several candidate loci
347 associated with root metaxylem phenes under well-watered and water stressed conditions by
348 integrating a GWAS conducted in maize with a root-specific gene co-expression network and by
349 performing a cross-species comparative GWAS with rice. We observed wide variation in root
350 metaxylem phenotypes in maize, and this variation is under distinct genetic control in optimal
351 and water-limited environments. We observed high heritability in root metaxylem phenes (Table
352 1). Broad-sense heritability observed was higher than previously reported values for root

353 anatomical phenes (Kadam et al., 2017; Schneider et al., 2020a), but may be slightly conflated
354 given that these values were based on only 95 genotypes than were planted in each season. Mean
355 values of all metaxylem phenes apart from volumetric flow rate were unchanged in response to
356 drought stress (Figure 1), but responses to drought varied by genotype (Supplemental Figure S1).
357 There were few genetic loci associated with root metaxylem phenes that co-localized between
358 water regimes (Supplemental Table S4, Figure 2, Figure 6A), which suggests that drought
359 induces changes in vascular patterning distinctly different from the processes employed when
360 water is more readily available. Unexpectedly, three times as many non-synonymous
361 consequences created by minor allele substitutions were associated with root metaxylem phenes
362 in the well-watered treatment compared to water stress (Figure 3). Modifications in plant
363 function due to a missense minor allele substitution may be more impactful under water stress
364 because of the greater selection pressure acting on these alleles compared to well-watered
365 conditions. The mechanisms counteracting potential functional impairments due to missense
366 mutation are perhaps more robust under water stress (Balestrazzi et al., 2011), leading to reduced
367 prevalence of missense variants compared to non-stressed conditions.

368 Our GWAS results identified several candidate genes associated with root metaxylem phenes
369 under well-watered and water stress conditions, and these candidate genes likely serve functional
370 roles relevant to xylem development according to the gene co-expression network. GWAS has
371 been widely utilized as a tool to identify genes related to a particular phenotype, but it also
372 presents many challenges. First, GWAS identifies many genes of which a notable proportion are
373 false positives. Instead of relying solely on significance values associated with SNPs, we sought
374 candidate genes with strong and consistent associations with root metaxylem phenotypes in
375 maize across two field seasons and in a cross-species GWAS comparison with rice. Second,
376 phenotyping highly complex quantitative traits associated with small effect sizes remains a
377 challenge in GWAS (Ingvarsson and Street, 2011; Schneider et al., 2020a; Schneider et al.,
378 2020b), which in turn makes candidate gene selection difficult. Integrating GWAS with a gene
379 co-expression network enables candidate gene selection to be determined by network
380 relationships inferring gene essentiality and biological function in its respective module (Yu et
381 al., 2004; Yu et al., 2007; McDermott et al., 2009). Of the 103 candidate genes identified through
382 GWAS that belonged to gene co-expression modules associated with root tissues most relevant
383 to xylem development, we identified 7 bottleneck genes, 9 hub genes, and 17 bottleneck/hub

384 genes (Figure 5, Supplemental Figure S5). We argue that these candidate genes that serve as hub
385 and/or bottleneck genes within a gene co-expression network merit greater attention for
386 validation in functional studies. Because these genes are more essential for maintaining gene-
387 gene interactions and signaling cascades, mutation of hub and bottleneck genes may have a
388 greater chance of inducing lethality. However, they also promise a higher likelihood of
389 producing substantial modification in phenotype and function.

390 Because of their contribution to xylem vessel wall development and reinforcement, genes
391 involved in cell wall processes are natural targets for further investigation. Three genes in xylem-
392 related co-expression modules are associated with cell wall-related processes and lignin
393 biosynthesis according to their Mapman annotation: alpha-L-arabinofuranosidase /beta-D-
394 xylosidase isoenzyme ARA-I (Zm00001d009060) associated with cell wall degradation,
395 pectinesterase (Zm00001d022567), and 4-coumarate--CoA ligase-like 4 (Zm00001d027519)
396 (Supplemental Table S3). Four additional candidate genes were proposed to be associated with
397 the biosynthesis and metabolism of cell-wall polysaccharides (Okekeogbu et al., 2019)
398 (Supplemental Table S3): a pectate lyase (Zm00001d015328), a chitin elicitor-binding protein
399 (Zm00001d027533), a protein disulfide isomerase (Zm00001d046399), and a glucan endo-1,3-β-
400 glucosidase (Zm00001d047712). Interestingly, all candidate genes in this group were associated
401 with root metaxylem size-related phenes under water stress. Surprisingly, we did not find any
402 significant associations with cell wall-related genes that are well known to directly influence
403 xylem development. For instance, cellulose synthase 4 (CesA4), which contained a SNP with a
404 consistent effect on phenotype that was just below the p-threshold ($-\log(p) = 3.02$), is a known
405 positive regulator of xylem differentiation in *Arabidopsis* (Taylor et al., 2003) and in turn is
406 regulated by VASCULAR-RELATED NAC DOMAIN7 (VND7) (Yamaguchi et al., 2011).
407 Much research has demonstrated that VND6 and VND7 are key regulators of xylem vessel
408 differentiation in *Arabidopsis* (Kubo et al., 2005; Yamaguchi et al., 2010a; Yamaguchi et al.,
409 2010b; Yamaguchi et al., 2011; Turco et al., 2019), but neither of these genes have yet been
410 characterized in maize. Maize homologs of VND6 – NAC10, NAC27, NAC46, NAC131 – and
411 VND7 – NAC62 and NAC92 – were co-expressed in the three modules strongly associated with
412 stele tissues 3 DAS (“lightcyan”, “thistle2”, “yellowgreen”), but none of these genes were
413 associated with significant SNPs detected in GWAS.

414 Several gene candidates associated with phytohormone biosynthesis and signaling were
415 identified in our GWAS analyses. Brassinosteroid-deficient *Arabidopsis* mutants were severely
416 dwarfed, exhibited impaired root elongation, and produced fewer xylem in leaf vascular bundles
417 (Szekeres et al., 1996; Choe et al., 1999a; Choe et al., 1999b). In our cross-species GWAS, two
418 additional gene candidates involved in brassinosteroid metabolism were associated with various
419 metaxylem vessel area-related phenes under WW in both maize and rice (Table 3). $\Delta(7)$ -sterol-
420 C(5)-desaturase (Zm00001d008569, Os01g0134500) is the rate-limiting step in brassinolide
421 biosynthesis and impairment of its activity is linked to defective longitudinal growth, irregularly
422 spaced vascular bundles, and reduced xylem vessel size and number (Choe et al., 1999b). An
423 additional gene syntenic pair (Zm00001d046838, Os06g0334300) encoding a putative receptor-
424 like kinase family protein sharing a high degree of homology to HERCULES1 (HERK1), which
425 is regulated by brassinosteroids and required for cell elongation (Guo et al., 2009a; Guo et al.,
426 2009b). The cross-species GWAS comparison also identified the syntenic gene pair for a
427 DnaJ/heat shock protein 40 family protein (Zm00001d039000/Os05g0562300) that was
428 significantly associated with maximum and median metaxylem vessel areas under well-watered
429 conditions and metaxylem vessel number in the rice *indica* subpopulation. Interestingly, a
430 member of this family has been shown to mediate environmental stress responses via
431 brassinosteroid signaling – over-expression of the gene maintained proper cell elongation in the
432 inflorescence and roots in the presence of a brassinosteroid inhibitor (Bekh-Ochir et al., 2013). In
433 the maize GWAS, five additional genes with potential associations with hormone metabolism
434 and biosynthesis were identified (Supplemental Table S3). A flavonol synthase
435 (Zm00001d002100) and AP2/EREB transcription factor 209 (EREB209) are involved in
436 ethylene metabolism and were significantly associated with total root metaxylem vessel area and
437 volumetric flow rate, respectively, under water stress. Ethylene has been shown in *Zinnia*
438 *elegans* cultures to play a dual role by stimulating the rate of tracheary element differentiation
439 and controlling the stem cell pool size during secondary xylem formation (Pesquet and
440 Tuominen, 2011). Auxin response factor 29 (ARF29) and aux/IAA-transcription factor 22
441 (IAA22) were significantly associated with various root metaxylem vessel size related
442 phenotypes under water stress and well-watered conditions, respectively. Auxin is a key
443 regulator of nearly every plant developmental process including many aspects of vascular
444 development (Milhinhos and Miguel, 2013). Most recently, auxin application was found to

445 repress transcription of NACs necessary for fiber and secondary cell wall development and
446 promote vessel-specific NACs in *Populus* stems (Johnsson et al., 2019). The function of these
447 gene candidates has been mostly characterized in shoots, but our results suggest they may also
448 contribute to variation in root metaxylem phenotypes.

449 Interestingly, the gene encoding a nodulin-like family protein (Zm00001d005082) contained 11
450 significant SNPs associated with maximum, median, and total metaxylem vessel areas and
451 volumetric flow rate under water stress and co-expressed with genes highly expressed in the root
452 meristematic/elongation zone 3 DAS (Supplemental Table S3). This nodulin lies within the
453 genomic region on chromosome 2 that was densely populated with SNPs strongly associated
454 with total root metaxylem vessel area under water stress and may also be a hub gene since its
455 closeness centrality was relatively high (Supplemental Figure S5). Another nodulin protein
456 (Zm00001d037160) contained one SNP strongly associated with metaxylem vessel number and
457 co-expressed with genes highly expressed in the stele 3 DAS (Supplemental Table S3). Nodulins
458 are not specific to legumes since homologs of nodulins have been found in several non-
459 nodulating species (Denancé et al., 2014). In non-nodulating species, nodulin-like proteins are
460 transmembrane proteins shown to transport a wide range of compounds and one has been shown
461 to enhance root hair elongation in rice (Huang et al., 2013). Zm00001d005082 belongs to a
462 nodulin-like protein subfamily whose transport specificity has yet to be characterized in plants
463 (Denancé et al., 2014). Our results suggest a potential novel role for nodulin and nodulin-like
464 proteins, which merits further investigation.

465 Though rice root metaxylem were not phenotyped under drought stress, we identified several
466 shared genetic loci that were directly or indirectly associated with drought responses. One
467 syntenic gene pair (Zm00001d048165/Os05g0562200) encodes the protein drought-induced 19
468 (Table 3), which is a transcriptional activator whose downregulation mutant resulted in longer
469 root systems and enhanced tolerance to drought and high salinity stress in *Arabidopsis* (Qin et
470 al., 2014). Interestingly, drought-induced 19 potentially interacts with ERD15 (Qin et al., 2014),
471 which was detected as another syntenic gene pair in the cross-species GWAS comparison.
472 ERD15 (Zm00001d048165/Os03g0353400), is rapidly activated under drought stress and is a
473 negative regulator of ABA (Kariola et al., 2006). ERD15 was also found to mediate osmotic
474 stress-induced programmed cell death in soybean (*Glycine max*) protoplasts (Alves et al., 2011).

475 Programmed cell death elicits xylem proliferation, so it is particularly intriguing that ERD15 is
476 associated with metaxylem vessel number in both maize and rice. Similarly, the activity of root
477 specific kinase 1 (Zm00001d014243/Os10g0395000), which was associated with volumetric
478 flow rate under well-watered conditions in maize and median vessel area in the *aus* rice
479 subpopulation (Table 3), is induced by dehydration and salt (Hwang and Goodman, 1995). The
480 maize GWAS also detected Zm00001d047710, a hypothetical gene of unknown function likely
481 involved in ABA synthesis and degradation, that was associated with total root metaxylem vessel
482 area under water stress (Supplemental Table S3). Though, it is surprising that more candidate
483 genes involved in ABA metabolism were not detected in the GWAS. ABA has only recently
484 been causally linked to induce changes in vascular development (Ramachandran et al., 2018) and
485 crosstalk with other phytohormones creates complex interactions. More research is needed to
486 investigate these relationships further.

487 Our findings suggest broadly that many genes influence root metaxylem phenotypes . In the
488 classic paradigm, many of the candidate genes proposed here may be validated with the use of
489 knockout or over-expression mutants to help elucidate the activity of these individual genes
490 relative to root metaxylem phenotypes and subsequent performance outcomes under drought.
491 However, while that strategy will certainly aid our fundamental understanding of vascular
492 development in a crop species, it may not ultimately be helpful for producers. Our results
493 indicate that identifying genetic loci advantageous in all environments may be difficult given the
494 low degree of overlap between watering regimes (Supplemental Table S4). Moving forward, it
495 may be wiser to develop new germplasm with multiplexed mutations predicted to better adapt to
496 an unpredictable environment. Given that many root phenotypes are influenced by many genes
497 with small effects (Schneider et al., 2020a; Schneider et al., 2020b) despite being highly heritable
498 (Table 1), stacking multiple mutations may elicit more substantial phenotypic differences.
499 Alternatively, we could assess the activity of our candidate genes in genotypes previously
500 demonstrated to be more drought tolerant. Furthermore, given our limited overlap between
501 species, a gene with demonstrated utility in one plant species may not prove to be equally as
502 beneficial in another. Several homologs of root-specific kinase 1
503 (Zm00001d014243/Os10g0395000) with high sequence similarity were identified in other
504 monocotyledonous species, but none were identified in a dicot (Figure 6). This suggests that the
505 structure and activity of root-specific kinase 1 may have evolved to be unique to monocots and

506 may not play a similar role in a dicotyledonous species. Therefore, we must expand our
507 understanding of the genetic mechanisms controlling vascular development into more model
508 systems. Vascular development specific to cereal crops has been largely overlooked and must be
509 better characterized in order to produce novel maize lines with hydraulic systems designed to
510 safeguard yields under stress.

511 In this study, root metaxylem phenotypes were observed in a panel of diverse maize lines
512 exposed to optimal and water-limited conditions. Substantial variation was observed for all
513 phenes measured in well-watered and water stressed conditions and these phenotypes were
514 heritable. In a GWAS, a substantial number of gene models contained SNPs significantly
515 associated with root metaxylem phenotypes under well-watered and water stress conditions. Few
516 genes co-localized in both treatments, indicating that the genetic mechanisms underlying root
517 metaxylem phenotypes are dependent on the environment. Integrating the GWAS results with a
518 root-specific gene co-expression network facilitated prioritization of candidate genes. We argue
519 that genes considered to be more essential in the network should be prioritized for validation.
520 Using a cross-species GWAS comparison, we found shared genetic architecture in root
521 metaxylem phenotypes, indicating that select genes may have conserved roles amongst species.
522 Identifying genes that regulate root metaxylem phenotypes will deepen our understanding of
523 plant vascular development, particularly in response to the environment, and provide novel
524 targets for plant breeders to develop cereal varieties best suited to water-limited environments.

525 **Materials and Methods**

526 *Plant Materials, Field Conditions and Experimental Design*

527 The root phenotypes of 180 and 412 maize (*Zea mays*) genotypes from the Wisconsin Diversity
528 Panel (Hansey et al., 2011; Hirsch et al., 2014) were evaluated in the field in 2015 and 2016,
529 respectively, under well-watered and water stressed conditions (Supplemental Table S1). The
530 Wisconsin Diversity Panel is a large collection of inbred maize lines of similar vigor
531 representing the genetic diversity of North American temperate maize. A subset of 95 genotypes
532 were grown in both 2015 and 2016. All experiments were conducted at the Apache Root Biology
533 Center (ARBC) located near Willcox, AZ, USA (32° 29 099 N, 109° 419 3099 W). Field trials
534 were conducted in a Grab loam soil (coarse-loamy, mixed, thermic Typic Torrifuvent) from
535 May through October in 2015 and 2016. Each genotype was planted in a single-row plot of 20

536 individuals per plot with 23 cm spacing between individuals. Rows were spaced 75 cm apart
537 (5.74 plants m⁻²). Two replications of the WiDiv were grown in each treatment in a randomized
538 complete block design. Experiments were irrigated using a center pivot irrigation system. Well-
539 watered and water stress treatments were induced in separate blocks. The water stress treatment
540 was induced four weeks after planting by withholding 50% of the water needed to sustain
541 adequate growth in the well-watered blocks. The severity of water stress was monitored over the
542 course of the season using PR2 multi-depth soil moisture probes (Dynamax, Houston, TX,
543 USA). Fertilizer and lime application were adjusted according to soil test results in order to meet
544 the nutritional demands for maize production. Pest and pathogen control were applied as needed.

545 *Field phenotypic data*

546 Maize root metaxylem phenotypes were evaluated using the shovelomics method (Trachsel et al.,
547 2010) coupled with laser ablation tomography (LAT) (Hall et al., 2019; Strock et al., 2019). To
548 summarize, the root crown of one representative maize plant was excavated from each plot just
549 prior to anthesis in a soil monolith using a standard spade approximately 30 cm wide and deep
550 and washed to remove the remaining soil. Samples to assess the root anatomy were collected by
551 excising two segments from the fourth whorl nodal root 5 to 8 cm from the base of the root. The
552 samples were preserved in 75% (v/v) ethanol in water and ablated using LAT. During LAT, the
553 root sample is placed on an imaging stage and moved into a 355 nm pulsed laser (Avia 7000) and
554 vaporized in the focal plane of a camera (Canon T3i with a MP-E 65mm micro lens) that
555 simultaneously captured an image of the cross-section. Metaxylem features were quantified in
556 each cross-section image using MIPAR software (Sosa et al., 2014). Two images were collected
557 from each root segment and averaged to assess the mean fourth nodal root metaxylem
558 phenotype. The theoretical volumetric flow rate was estimated based on the dimensions and
559 number of metaxylem vessels present in each image using the Exact equations (Berker, 1963;
560 Lewis and Boose, 1995), which estimates the volumetric movement of water through non-
561 circular conduits.

562 Broad-sense heritability and repeatability on an entry mean basis of each metaxylem phenone was
563 estimated according to (Fehr, 1991). Marker-based heritability was calculated using the
564 'heritability' v.1.3 R package (Kruijer, 2019).

565 *Assembly of a root gene co-expression network*

566 Co-expression analysis and module identification were conducted on a publicly available RNA-
567 Seq dataset collected on 19 samples comprising multiple tissues and timepoints (Supplemental
568 Table S6) (Stelplflug et al., 2016) using the WGCNA R package (Langfelder and Horvath, 2008).
569 Genes with an FPKM < 1 for all samples were omitted from the WGCNA analysis. Parameters
570 were adjusted so that the soft threshold was selected to produce a >90% model fit. Additionally,
571 a minimum module size was 30 and the branch cut height was set to 0.8. Modules with a high
572 likelihood to be related to xylem development were designated as those displaying high average
573 gene expression in the stele (Stele_3d), differentiation zone (DifferentiationZone_3d),
574 meristematic/elongation zone (Mz.Ez_3d), whole root system (WholeRootSystem_3d) 3 days
575 after sowing (DAS), and zones 1 and 2 of the primary root 7 DAS (TapRoot_Z1_7d,
576 TapRoot_Z2_7d). Gene ontology (GO) enrichment was conducted on each xylem-related
577 module using AgriGO (Du et al., 2010) to correlate possible biological roles with xylem
578 development.

579 Network topology metrics were calculated to infer the relationship between each gene and the
580 rest of the network. For each gene, closeness centrality, i.e. the inverse of the average shortest
581 path between the gene of interest and all other nodes in the network, and betweenness centrality,
582 i.e. the number of shortest paths between all pairs of nodes in the network that pass through the
583 gene of interest, were calculated using 'igraph' (Csardi and Nepusz, 2006). Genes in the
584 uppermost quintile of closeness centrality and betweenness centrality were selected as hub and
585 bottleneck genes, respectively. Genes may be labeled as both a hub and bottleneck. Network
586 interactions were visualized using Cytoscape 3.8.0 (Lopes et al., 2010).

587 *Genome-wide association analysis*

588 GWAS was performed using the phenotypic values obtained from each season and treatment and
589 a panel of 899,784 SNPs assembled using RNA-Seq data from whole seedlings of each member
590 of the WiDiv (Mazaheri et al., 2019) implemented in the GAPIT package (Lipka et al., 2012) in
591 R. Single nucleotide polymorphisms (SNPs) with minor allele frequencies less than 0.01 were
592 discarded from the panel. Due to differences in taxa membership between each season, the
593 number of SNPs included in each GWAS differed: 578,279 in 2015 and 574,175 in 2016. The
594 first three principal components were used as covariates to control for population structure. The
595 minor allele effects associated with SNPs observed in the 2016 GWAS were tested using the

596 2015 GWAS to identify SNPs with consistent minor allele effects in both seasons. The
597 significance threshold was selected using a linear model that predicts a significant p-threshold
598 according to the marker-based heritability (Kaler and Purcell, 2019). Using the mean marker-
599 based heritability of all phenes (0.264), the p-threshold was predicted to be at $-\log(p) \leq 3.43$. A
600 SNP that satisfied the p-threshold in 2016 and displayed consistent minor allele effects in both
601 seasons was designated as “significant.” Candidate genes corresponding to a significant SNP
602 were detected according to the AGPv4 reference sequence assembly (Jiao et al., 2017).
603 Annotation of candidate genes was obtained from MaizeGDB (Portwood et al., 2018).

604 *Comparative GWAS between Maize and Rice*

605 GWAS was conducted on rice metaxylem phenes grown under well-watered conditions in the
606 greenhouse (Reeger et al., unpublished). Rice root anatomy was evaluated on 336 rice (*Oryza*
607 *sativa*) accessions from the Rice Diversity Panel 1 (RDP1) (Zhao et al., 2011) grown in
608 greenhouses at University Park, PA (40°49' N, 77°52' W). Accessions represented all *O. sativa*
609 subpopulations: 52 *aus*, 67 *indica*, 11 *aromatic*, 74 *temperate japonica*, 80 *tropical japonica*, and
610 51 admixed accessions. Plants were grown in 10.5 L pots (21 cm x 40.6 cm, top diameter x
611 height, Nursery Supplies Inc., Chambersburg, PA, USA) filled with growth medium consisting
612 of 40% v/v medium size (0.3-0.5 mm) commercial grade sand (Quikrete Companies Inc.,
613 Harrisburg, PA, USA), 60% v/v horticultural vermiculite (Whittemore Companies Inc.,
614 Lawrence, MA, USA), and solid-phase buffered phosphorus (Al-P, prepared according to (Lynch
615 et al., 1990)) providing a constant availability of high (100 μ M) phosphorus concentration in the
616 soil solution. Each pot was direct-seeded with three seeds, and after 7 days plants were thinned to
617 one per pot. Plants were irrigated once per day via drip irrigation with Yoshida nutrient solution
618 without phosphate (Yoshida et al., 1971), which was adjusted to pH 5.5-6.0 daily. At the 8th leaf
619 stage, root systems of each plant were excavated, washed with water, and preserved in 70% (v/v)
620 ethanol in water for later sampling. Preserved root tissue at 15 cm from the root apex of two
621 nodal roots was freehand sectioned under a dissection microscope (SMZ-U, Nikon, Tokyo,
622 Japan) at 4x magnification using Teflon-coated double-edged stainless steel blades (Electron
623 Microscopy Sciences, Hatfield, PA, USA). Images of the root cross-section were captured using
624 a Diaphot inverted light microscope (SMZ-U, Nikon, Tokyo, Japan) at 40x magnification
625 equipped with digital camera (NIKON DS-Fi1, Tokyo, Japan). The two best images were

626 selected to quantify root anatomy using the image analysis software Rice Root Analyzer
627 (Taeparsartsit 2013, unpublished) to measure the number of metaxylem vessels and RootScan
628 software (Burton et al., 2012) to measure metaxylem vessel area. Mean values of each root
629 anatomical phenon for each genotype were calculated and used for all further analysis.

630 Using the 4.8 million SNPs from the Rice Reference Panel (RICE-RP) (Wang et al., 2018),
631 genome-wide associations were calculated for root anatomical traits in all individuals (ALL), as
632 well as within subpopulations (*indica*, *IND*; *tropical-japonica*, *TRJ*; *temperate-japonica*, *TEJ*;
633 *aus*, *AUS*). To avoid false-positives and reduce computational requirements per association, the
634 SNPs were divided into 6 non-orthogonal subsets by linkage-disequilibrium (r^2) pruning using
635 the *indep* and *indep_pairwise* functions in plink1.9 (Chang et al., 2015). A linear mixed-model in
636 the *gwas()* function of the ‘rrBLUP’ package in R was used for all associations (Endelman,
637 2011). A minimum minor-allele frequency of 0.05 was used (min.MAF = 0.05) with at least 3
638 minor allele count, and variance components were calculated once (P3D = TRUE). Based on
639 previous methods (McCouch et al., 2016), no principle components were used for single
640 subpopulations, but three principle components were added for associations in ALL (n.PC = 3).
641 To identify genomic regions in the output, the following requirements were used: region had
642 greater than 3 SNPs with $-\log(p) > 4$ that were within 200 kb of each other, region was
643 significant in at least 5 of 6 SNP subsets, and the most-significant SNP (MS-SNP) in the region
644 had $-\log(p) > 5$. In total, 3636 candidate genes were detected in rice for median metaxylem area
645 and number of metaxylem vessels. Genes within these regions with their GO names were
646 retrieved using Bioconductor tools in R (Huber et al., 2015).

647 Maize and rice syntenic genes were identified using the EnsemblPlants database of homologs via
648 the biomaRt package in R (Huber et al., 2015), which utilizes a synteny method based on
649 orthology that was previously described (Schnable et al., 2009). Syntenic gene pairs most likely
650 associated with root metaxylem phenes were made up of genes with a significant association in
651 both maize ($-\log(p) > 3.43$) and rice ($-\log(p) > 4$) GWAS. Significant allelic effects on maize
652 root metaxylem phenotypes were determined using a two-sample t-test ($\alpha < 0.05$). Because rice
653 candidate genes may be distant from the significant SNP associated with a root metaxylem
654 phenon, haplotypes of each candidate gene were identified using a cluster analysis and their
655 metaxylem root phenotypes were compared. SNP genotypes across accessions, which included

656 all nonsynonymous SNPs in the candidate gene as determined by the SNP-Seek database
657 (Mansueto et al., 2017), were clustered into similar groups using K-means clustering via the
658 ‘pheatmap’ v1.0.12 package in R (Kolde, 2015), where the number of clusters was determined
659 using the within sums of squares method. Significant differences in rice root metaxylem
660 phenotypes across haplotypes were determined using Kruskal-Wallis and pairwise Wilcoxon
661 multiple comparison tests ($\alpha < 0.05$). Phylogenetic trees based on syntenic gene pairs were
662 constructed to infer the evolutionary history. Sequences of high similarity (megablast) to the
663 maize gene were identified using BLAST and their amino acid sequences were aligned using the
664 MUSCLE algorithm in MEGA X (Hall, 2013). All positions with less than 95% site coverage
665 were eliminated. A bootstrap consensus tree was constructed from 500 replications of Maximum
666 Likelihood trees in MEGA X (Hall, 2013) and edited in TreeGraph 2 (Stöver and Müller, 2010).
667 The percentage of replicate trees in which the associated taxa clustered together is shown next to
668 the branches.

669 *Data Analysis*

670 All data analyses were performed in R version 4.0.0 (R Core Team, 2020) with graphical
671 illustration using ‘ggplot2’ (Wickham, 2016).

672 **Supplemental Data**

673 Supplemental Table S1. Genotypes of the Wisconsin Diversity Panel grown in 2015 and 2016.

674 Supplemental Table S2. Number of SNPs exhibiting consistent effects on root phenotypes in
675 each treatment across both seasons.

676 Supplemental Table S3. Significant SNPs and candidate genes identified via GWAS for
677 associated with all root metaxylem phenes under well-watered and water stress conditions.
678 MXAmax, maximum root metaxylem vessel area; MXAmed, median root metaxylem vessel
679 area; MXAtot, total root metaxylem vessel area; MXN, metaxylem vessel number; VFR,
680 volumetric flow rate.

681 Supplemental Table S4. Significant SNPs and candidate genes that were associated with root
682 metaxylem phenes in both well-watered (WW) and water stress (WS) conditions. MXAmax,

683 maximum root metaxylem vessel area; MXAmed, median root metaxylem vessel area; MXAtot,
684 total root metaxylem vessel area; MXN, metaxylem vessel number; VFR, volumetric flow rate.

685 Supplemental Table S5. Statistics describing network topology and membership size for each co-
686 expression module strongly associated with root tissues relevant to root metaxylem development.

687 Supplemental Table S6. List of 19 root tissues used to build the root-specific gene co-expression
688 network.

689 Supplemental Figure S1. Correlations between mean values of each genotype under well-watered
690 (WW) and water stressed (WS) conditions for each metaxylem phene in 2015 (black) and 2016
691 (grey). The solid black or grey lines indicate the slope of the correlation. The solid blue line
692 indicates where $x = y$.

693 Supplemental Figure S2. Q-Q plots assessing the fitness of the model for GWAS of root
694 metaxylem phenes under well-watered (WW) and water stress (WS) conditions.

695 Supplemental Figure S3. General outline of the filtering steps used to identify SNPs with
696 consistent allelic effects in separate GWAS conducted with data collected in 2015 and 2015. (A)
697 A substantial proportion of the SNP panel was included in each GWAS. Binned scatterplots
698 showing (B) the full SNP panel and (C) the filtered set containing SNPs of consistent minor
699 allele effects. The gradation of the bin corresponds to the number of SNPs residing in the bin
700 where densely populated bins are light blue while more sparsely populated bins are dark blue.

701 Supplemental Figure S4. Mapman ontogenic categories for annotated gene models associated
702 with significant SNPs in well-watered and water stress conditions.

703 Supplemental Figure S5. Network topology metrics used to identify hub and bottleneck genes in
704 the pool of candidate genes identified via GWAS. Scatterplots showing closeness centrality
705 against betweenness centrality of each gene for the remaining gene co-expression modules most
706 strongly associated with root tissues relevant to metaxylem development. Modules
707 “navajowhite2” and “thistle1” did not contain any significant SNPs detected in the GWAS.
708 Colors correspond to bottleneck (BN, red), bottleneck/hub (BN/HUB, yellow), hub (HUB, blue),
709 and non-affiliated (None, grey) genes.

710 Supplemental Figure S6. Haplotypes of rice genes encoding a root-specific kinase 1
711 (Os10g0395000).

712 **Acknowledgements**

713 This research was supported by the National Institute of Food and Agriculture, U.S. Department
714 of Agriculture, award #2017-67013-26192 and Hatch project 4732, and the Howard G. Buffett
715 Foundation. We thank Robert Snyder and Patricio Cid for technical support; and Charles
716 Anderson, Ivan Baxter Brian Dilkes, and Jesse Lasky for helpful discussions.

717 **Tables**

718

719 Table 1. Two-way ANOVA of root metaxylem phenes measured across two field seasons under
 720 well-watered (WW) and water stress (WS) conditions, and broad-sense and marker-based
 721 heritabilities calculated for each phene among 95 genotypes planted in each season.
 722 Repeatability of each phene was calculated using all genotypes grown in each season. Bold
 723 numbers in the two-way ANOVA indicate significant associations ($p < 0.05$).

Phene Description	Two-Way ANOVA						Broad-sense heritability (95 genos)	Marker-based heritability (95 genos)	Repeatability 2015 (180 genos)	Repeatability 2016 (412 genos)
	Year		Trt		Year*Trt					
	F	p	F	p	F	p				
Maximum individual metaxylem vessel area (mm ²)	8.077	0.00456	3.19 2	0.074 2	3.197	0.07 4	0.625	0.327	0.652	0.67
Median individual metaxylem vessel area (mm ²)	5.769	0.0165	1.23 4	0.267	1.236 4	0.26 6	0.805	0.361	0.668	0.662
Total metaxylem vessel area (mm ²)	0.000 9	0.976	0.23 7	0.627	0.238 6	0.62 5	0.646	0.133	0.602	0.466
Metaxylem vessel number	8.661	0.00332	0.59 2	0.442	0.590 6	0.44 2	0.672	0.251	0.827	0.502
Volumetric flow rate (mm ³ /s)	11.31 4	0.000794	4.41 2	0.035 9	4.410 9	0.03 6	0.72	0.249	0.8	0.527

724

725

726 Table 2. Number of significant SNPs and candidate genes detected in the maize GWAS and the
 727 number of candidate genes found in one of 14 gene co-expression modules associated with root
 728 tissues most relevant to xylem development.

Phene	Treatment	Number of Significant SNPs	Number of Gene Models within 5kb of significant SNP	Number of Genes in Xylem-Related Co-expression Modules
Maximum root metaxylem vessel area	WW	43	26	18
	WS	53	43	19
Median root metaxylem vessel area	WW	70	44	13
	WS	60	29	21
Total root metaxylem vessel area	WW	21	20	8
	WS	59	35	11
Metaxylem vessel number	WW	51	29	16
	WS	29	22	9
Volumetric flow rate	WW	29	22	10
	WS	39	22	5
Total	WW	181	124	57
	WS	176	126	50
	Total	351	244	103

729

730

731 Table 3. Syntenic gene pairs that were strongly associated with root metaxylem phenes in both
 732 maize and rice.

Maize Gene	Maize Root Phene	Rice Gene	Rice Root Phene	Rice Subpopulation	Description
Zm00001d008569	MXAtot_WW, VFR_WW	Os01g0134500	MXAmed	IND	Delta(7)-sterol-C5(6)-desaturase 1
Zm00001d011147	MXAmax_WS	Os09g0570400	MXN	ALL	Ascorbate transporter, chloroplastic
Zm00001d014243	VFR_WW	Os10g0395000	MXAmed	AUS	root-specific kinase 1
Zm00001d017216	MXAtot_WW	Os02g0617700	MXAmed	IND	Polyribonucleotide nucleotidyltransferase 2, mitochondrial
Zm00001d038999	MXAmax_WW, MXAmed_WW	Os05g0562200	MXN	IND	drought-induced 19
Zm00001d039000	MXAmax_WW, MXAmed_WW	Os05g0562300	MXN	IND	HSP40/DnaJ peptide-binding protein
Zm00001d046838	MXAmed_WW, MXAtot_WW	Os06g0334300	MXAmed	ALL	Putative receptor-like protein kinase family protein
Zm00001d048165	MXN_WS	Os03g0353400	MXN	ALL	EARLY RESPONSIVE TO DEHYDRATION 15 (ERD15)

733

734

735 **Figure Legends**

736 Figure 1. Wide variation exists in metaxylem phenes under well-watered and water stress
737 conditions in the field. (A) Violin plots show the distribution of each metaxylem phene under
738 well-watered (WW, blue) and water stress (WS, red) in each field season while the overlaid box
739 plots show the median bounded by the first and third quartile. Two-way ANOVA determined
740 statistical differences between treatments and growth seasons (Table 1). (B) Root cross-sectional
741 images collected via laser ablation tomography illustrate the range in each metaxylem
742 phenotype. White scale bars in the bottom left of each image are equal to 0.5 mm.

743 Figure 2. Manhattan plots of the results of the GWAS for (A) maximum metaxylem vessel area,
744 (B) median metaxylem vessel area , (C) total metaxylem vessel area, (D) metaxylem vessel
745 number and (E) volumetric flow rate in each watering regime in 2016 (grey). Results from the
746 well-watered studies are shown on the positive axis while the water stress is on the negative axis.
747 The dotted line indicates the significance threshold ($-\log(p) > 3.43$). Dots colored blue and red
748 are significant SNPs with consistent allelic effects in the 2015 GWAS in the well-watered and
749 water-stressed treatments, respectively. Select genomic regions that shared significant SNPs in
750 both treatments have been highlighted in purple.

751 Figure 3. Predicted consequences of minor allele variants presented as a proportion of the total
752 number of significant SNPs in well-watered (WW) and water stressed (WS) conditions.

753 Figure 4. A gene co-expression network and significant correlation of modules. (A) Hierarchical
754 clustering dendrogram displaying 39 modules of co-expressed genes. (B) A heatmap showing the
755 significance of the correlation ($-\log(p)$) between modules and various root tissues. (C) Inferred
756 biological function of modules most likely associated metaxylem development based on GO
757 analysis. Only GO terms most relevant to xylem development are displayed. No GO terms were
758 over-represented by modules “lightcyan1”, “salmon4”, and “thistle1”.

759 Figure 5. Gene co-expression subnetworks for modules associated with root stele 3 days after
760 sowing. These modules were “lightcyan” (A, D), “thistle2” (B, E) and “yellowgreen” (C, F).
761 Network visualizations (A, B, C) show all interactions within the subnetwork. Scatterplots (D, E,
762 F) show the calculated closeness centrality and betweenness centrality for candidate genes
763 determined by GWAS residing in the corresponding module. All bottleneck (BN),

764 bottleneck/hub (BN/HUB) and hub (HUB) genes are shown in red, yellow, and blue,
765 respectively.

766 Figure 6. Comparative GWAS between maize and rice for metaxylem phenes identified a
767 syntenic gene pair encoding root-specific kinase 1 associated with root metaxylem phenotypes.
768 (A) Comparison of the results of three GWAS seeking genetic loci associated with root
769 metaxylem phenes in maize under well-watered (WW) and water-stressed (WS) conditions and
770 rice. (B) Manhattan plot of SNPs and their associated with the volumetric flow rate under WW
771 on maize chromosome 5 highlighting the candidate gene (Zm00001d014243) in red. (C)
772 Manhattan plot of SNPs associated with metaxylem vessel area on rice chromosome 10
773 highlighting the candidate gene (Os10g0395000) in red. (D) Significant differences in volumetric
774 flow rate in WW are associated with the minor allele (ALT, yellow) compared to the major allele
775 (REF, blue) determined by two-sample *t*-test ($p < 0.001$). (E) Significant differences in
776 metaxylem vessel area are associated with nine haplotypes of Os10g0395000 determined by
777 Kruskal-Wallis ($p < 0.001$). Haplotypes are disclosed in Supplemental Figure S6. (F)
778 Representative images maize root cross-sections captured via LAT illustrating visual phenotypic
779 differences in individuals that contained the minor (ALT) and major (REF) alleles. (G)
780 Representative images of rice root cross-sections collected by hand-sectioning illustrating visual
781 contrasts in metaxylem vessel area. (H) Phylogenetic tree of gene homologous to root-specific
782 kinase 1. The amino acid sequences of 28 proteins of high sequence similarity were aligned by
783 MUSCLE and the phylogenetic tree was constructed using MEGA version 10.1.8 and TreeGraph
784 2. Bootstrap values from 500 replicates were used to assess the robustness of the tree. The maize
785 and rice candidate genes identified in GWAS are labeled in bold.

786

787 **References**

- 788 **Abd Allah AA, Badawy SA, Zayed BA, El. Gohary AA** (2010) The Role of Root System
789 Traits in the Drought Tolerance of Rice (*Oryza sativa* L.). *International Journal of*
790 *Agricultural and Biological Sciences* **1**: 83–87
- 791 **Alves MS, Reis PAB, Dadalto SP, Faria JAQA, Fontes EPB, Fietto LG** (2011) A novel
792 transcription factor, ERD15 (Early Responsive to Dehydration 15), connects endoplasmic
793 reticulum stress with an osmotic stress-induced cell death signal. *J Biol Chem* **286**: 20020–
794 20030
- 795 **Balestrazzi A, Confalonieri M, Macovei A, Donà M, Carbonera D** (2011) Genotoxic stress
796 and DNA repair in plants: emerging functions and tools for improving crop productivity.
797 *Plant Cell Rep* **30**: 287–295
- 798 **Bekh-Ochir D, Shimada S, Yamagami A, Kanda S, Ogawa K, Nakazawa M, Matsui M,**
799 **Sakuta M, Osada H, Asami T, et al** (2013) A novel mitochondrial DnaJ/Hsp40 family
800 protein BIL2 promotes plant growth and resistance against environmental stress in
801 brassinosteroid signaling. *Planta* **237**: 1509–1525
- 802 **Bennetzen JL, Freeling M** (1997) The unified grass genome: synergy in synteny. *Genome Res*
803 **7**: 301–306
- 804 **Berker R** (1963) Intégration des équations du mouvement d'un fluide visqueux incompressible.
805 *Handbuch der Physik* **3**: 1–384
- 806 **Buell CR, Yuan Q, Ouyang S, Liu J, Zhu W, Wang A, Maiti R, Haas B, Wortman J, Pertea**
807 **M, et al** (2005) Sequence, annotation, and analysis of synteny between rice chromosome 3
808 and diverged grass species. *Genome Res* **15**: 1284–1291
- 809 **Burridge JD, Rangarajan H, Lynch JP** (2020) Comparative phenomics of annual grain legume
810 root architecture. *Crop Sci* 1–20
- 811 **Burton AL, Williams M, Lynch JP, Brown KM** (2012) RootScan: Software for high-
812 throughput analysis of root anatomical traits. *Plant Soil* **357**: 189–203
- 813 **Carpita NC** (1996) Structure and biogenesis of the cell walls of grasses. *Annual Reviews in*
814 *Plant Physiology Plant Molecular Biology* **47**: 445–476
- 815 **Chang CC, Chow CC, Tellier LC, Vattikuti S, Purcell SM, Lee JJ** (2015) Second-generation
816 PLINK: rising to the challenge of larger and richer datasets. *Gigascience* **4**: 1–16
- 817 **Chen W, Wang W, Peng M, Gong L, Gao Y, Wan J, Wang S, Shi L, Zhou B, Li Z, et al**
818 (2016) Comparative and parallel genome-wide association studies for metabolic and
819 agronomic traits in cereals. *Nature Communications* **7**: 1–10
- 820 **Chimungu JG, Brown KM, Lynch JP** (2014a) Large root cortical cell size improves drought
821 tolerance in maize. *Plant Physiol* **166**: 2166–2178

- 822 **Chimungu JG, Brown KM, Lynch JP** (2014b) Reduced root cortical cell file number improves
823 drought tolerance in maize. *Plant Physiol* **166**: 1943–1955
- 824 **Choe S, Dilkes BP, Gregory BD, Ross AS, Yuan H, Noguchi T, Fujioka S, Takatsuto S,**
825 **Tanaka A, Yoshida S, et al** (1999a) The Arabidopsis dwarf1 mutant is defective in the
826 conversion of 24-methylenecholesterol to campesterol in brassinosteroid biosynthesis. *Plant*
827 *Physiol* **119**: 897–907
- 828 **Choe S, Noguchi T, Fujioka S, Takatsuto S, Tissier CP, Gregory BD, Ross AS, Tanaka A,**
829 **Yoshida S, Tax FE, et al** (1999b) The Arabidopsis dwf7/ste1 mutant is defective in the
830 delta7 sterol C-5 desaturation step leading to brassinosteroid biosynthesis. *Plant Cell* **11**:
831 207–221
- 832 **Comas LH, Becker SR, Cruz VMV, Byrne PF, Dierig DA** (2013) Root traits contributing to
833 plant productivity under drought. *Front Plant Sci* **4**: 1–16
- 834 **Csardi G, Nepusz T** (2006) The igraph software package for complex network research.
835 *InterJournal, Complex Systems* 1695
- 836 **Dai A** (2013) Increasing drought under global warming in observations and models. *Nat Clim*
837 *Chang* **3**: 52–58
- 838 **Daryanto S, Wang L, Jacinthe P-A** (2016) Global Synthesis of Drought Effects on Maize and
839 Wheat Production. *PLoS One* **11**: e0156362
- 840 **Denancé N, Szurek B, Noël LD** (2014) Emerging functions of nodulin-like proteins in non-
841 nodulating plant species. *Plant Cell Physiol* **55**: 469–474
- 842 **Du Z, Zhou X, Ling Y, Zhang Z, Su Z** (2010) agriGO: a GO analysis toolkit for the
843 agricultural community. *Nucleic Acids Res* **38**: W64–70
- 844 **Endelman JB** (2011) Ridge regression and other kernels for genomic selection with R package
845 rrBLUP. *Plant Genome* **4**: 250–255
- 846 **Fehr W** (1991) *Principles of Cultivar Development: Theory and Technique*. Iowa State
847 University
- 848 **Feng W, Lindner H, Robbins NE 2nd, Dinneny JR** (2016) Growing Out of Stress: The Role
849 of Cell- and Organ-Scale Growth Control in Plant Water-Stress Responses. *Plant Cell* **28**:
850 1769–1782
- 851 **Finkelstein R** (2013) Abscisic Acid synthesis and response. *In* C Somerville, E Meyerowitz,
852 eds, *The Arabidopsis Book*. pp 1–36
- 853 **Gao Y, Lynch JP** (2016) Reduced crown root number improves water acquisition under water
854 deficit stress in maize (*Zea mays* L.). *J Exp Bot* **67**: 4545–4557
- 855 **Guet J, Fichot R, Lédée C, Laurans F, Cochard H, Delzon S, Bastien C, Brignolas F** (2015)
856 Stem xylem resistance to cavitation is related to xylem structure but not to growth and

- 857 water-use efficiency at the within-population level in *Populus nigra* L. *J Exp Bot* **66**: 4643–
858 4652
- 859 **Guo H, Li L, Ye H, Yu X, Algreen A, Yin Y** (2009a) Three related receptor-like kinases are
860 required for optimal cell elongation in *Arabidopsis thaliana*. *Proc Natl Acad Sci U S A* **106**:
861 7648–7653
- 862 **Guo H, Ye H, Li L, Yin Y** (2009b) A family of receptor-like kinases are regulated by BES1 and
863 involved in plant growth in *Arabidopsis thaliana*. *Plant Signal Behav* **4**: 784–786
- 864 **Hacke UG, Sperry JS** (2001) Functional and ecological xylem anatomy. *Perspect Plant Ecol*
865 *Evol Syst* **4**: 97–115
- 866 **Hall BG** (2013) Building phylogenetic trees from molecular data with MEGA. *Mol Biol Evol*
867 **30**: 1229–1235
- 868 **Hall B, Lanba A, Lynch J** (2019) Three-dimensional analysis of biological systems via a novel
869 laser ablation technique. *J Laser Appl* **31**: 022602
- 870 **Hansey CH, Johnson JM, Sekhon RS, Kaeppler SM, de Leon N** (2011) Genetic diversity of a
871 maize association population with restricted phenology. *Crop Sci* **51**: 704–715
- 872 **Henry A, Cal AJ, Batoto TC, Torres RO, Serraj R** (2012) Root attributes affecting water
873 uptake of rice (*Oryza sativa*) under drought. *J Exp Bot* **63**: 4751–4763
- 874 **Hirsch CN, Foerster JM, Johnson JM, Sekhon RS, Muttoni G, Vaillancourt B,**
875 **Peñagaricano F, Lindquist E, Pedraza MA, Barry K, et al** (2014) Insights into the maize
876 pan-genome and pan-transcriptome. *Plant Cell* **26**: 121–135
- 877 **Hochholdinger F** (2009) The Maize Root System: Morphology, Anatomy, and Genetics.
878 *Handbook of Maize: Its Biology*. Springer New York, pp 145–160
- 879 **Ho MD, Rosas JC, Brown KM, Lynch JP** (2005) Root architectural tradeoffs for water and
880 phosphorus acquisition. *Funct Plant Biol* **32**: 737–748
- 881 **Hose E, Steudle E, Hartung W** (2000) Abscisic acid and hydraulic conductivity of maize roots:
882 a study using cell- and root-pressure probes. *Planta* **211**: 874–882
- 883 **Huang J, Kim CM, Xuan Y-H, Park SJ, Piao HL, Je BI, Liu J, Kim TH, Kim B-K, Han C-**
884 **D** (2013) OsSNBP1, a Sec14-nodulin domain-containing protein, plays a critical role in root
885 hair elongation in rice. *Plant Mol Biol* **82**: 39–50
- 886 **Huber W, Carey VJ, Gentleman R, Anders S, Carlson M, Carvalho BS, Bravo HC, Davis**
887 **S, Gatto L, Girke T, et al** (2015) Orchestrating high-throughput genomic analysis with
888 Bioconductor. *Nat Methods* **12**: 115–121
- 889 **Ingvarsson PK, Street NR** (2011) Association genetics of complex traits in plants: Tansley
890 review. *New Phytol* **189**: 909–922
- 891 **IPCC** (2013) *Climate Change 2013: The Physical Science Basis. Contribution of Working*

- 892 Group I to the Fifth Assessment Report of the Intergovernmental Panel on Climate Change.
893 Cambridge University Press
- 894 **Jaramillo RE, Nord EA, Chimungu JG, Brown KM, Lynch JP** (2013) Root cortical burden
895 influences drought tolerance in maize. *Ann Bot* **112**: 429–437
- 896 **Jeong H, Mason SP, Barabási A-L, Oltvai ZN** (2001) Lethality and centrality in protein
897 networks. *Nature* **411**: 41–42
- 898 **Jiao Y, Peluso P, Shi J, Liang T, Stitzer MC, Wang B, Campbell MS, Stein JC, Wei X,**
899 **Chin C-S, et al** (2017) Improved maize reference genome with single-molecule
900 technologies. *Nature* **546**: 524–527
- 901 **Johnsson C, Jin X, Xue W, Dubreuil C, Lezhneva L, Fischer U** (2019) The plant hormone
902 auxin directs timing of xylem development by inhibition of secondary cell wall deposition
903 through repression of secondary wall NAC-domain transcription factors. *Physiol Plant* **165**:
904 673–689
- 905 **Kadam NN, Tamilselvan A, Lawas LMF, Quinones C, Bahuguna RN, Thomson MJ,**
906 **Dingkuhn M, Muthurajan R, Struik PC, Yin X, et al** (2017) Genetic Control of Plasticity
907 in Root Morphology and Anatomy of Rice in Response to Water Deficit. *Plant Physiol* **174**:
908 2302–2315
- 909 **Kadam NN, Yin X, Bindraban PS, Struik PC, Jagadish KSV** (2015) Does morphological and
910 anatomical plasticity during the vegetative stage make wheat more tolerant of water deficit
911 stress than rice? *Plant Physiol* **167**: 1389–1401
- 912 **Kaler AS, Purcell LC** (2019) Estimation of a significance threshold for genome-wide associated
913 studies. *BMC Genomics* **20**: 1–8
- 914 **Kano M, Inukai Y, Kitano H, Yamauchi A** (2011) Root plasticity as the key root trait for
915 adaptation to various intensities of drought stress in rice. *Plant Soil* **342**: 117–128
- 916 **Kariola T, Brader G, Helenius E, Li J, Heino P, Palva ET** (2006) EARLY RESPONSIVE TO
917 DEHYDRATION 15, a negative regulator of abscisic acid responses in Arabidopsis. *Plant*
918 *Physiol* **142**: 1559–1573
- 919 **Klein SP, Schneider HM, Perkins AC, Brown KM, Lynch JP** (2020) Multiple Integrated
920 Root Phenotypes Are Associated with Improved Drought Tolerance. *Plant Physiol* **183**:
921 1011–1025
- 922 **Kolde R** (2015) pheatmap: Pretty heatmaps.
- 923 **Kruijer W** (2019) heritability: Marker-Based Estimation of Heritability Using Individual Plant
924 or Plot Data.
- 925 **Kubo M, Udagawa M, Nishikubo N, Horiguchi G, Yamaguchi M, Ito J, Mimura T, Fukuda**
926 **H, Demura T** (2005) Transcription switches for protoxylem and metaxylem vessel
927 formation. *Genes Dev* **19**: 1855–1860

- 928 **Langfelder P, Horvath S** (2008) WGCNA: an R package for weighted correlation network
929 analysis. *BMC Bioinformatics* **9**: 1–13
- 930 **Lewis AM, Boose ER** (1995) Estimating Volume Flow Rates Through Xylem Conduits. *Am J*
931 *Bot* **82**: 1112–1116
- 932 **Liakat Ali M, Luetchens J, Nascimento J, Shaver TM, Kruger GR, Lorenz AJ** (2015)
933 Genetic variation in seminal and nodal root angle and their association with grain yield of
934 maize under water-stressed field conditions. *Plant and Soil* **397**: 213–225
- 935 **Li H, Zhang D, Wang X, Li H, Rengel Z, Shen J** (2018) Competition between *Zea mays*
936 genotypes with different root morphological and physiological traits is dependent on
937 phosphorus forms and supply patterns. *Plant Soil* **434**: 125–137
- 938 **Lipka AE, Tian F, Wang Q, Peiffer J, Li M, Bradbury PJ, Gore MA, Buckler ES, Zhang Z**
939 (2012) GAPIT: genome association and prediction integrated tool. *Bioinformatics* **28**: 2397–
940 2399
- 941 **Lobell DB, Roberts MJ, Schlenker W, Braun N, Little BB, Rejesus RM, Hammer GL**
942 (2014) Greater sensitivity to drought accompanies maize yield increase in the U.S. Midwest.
943 *Science* **344**: 516–519
- 944 **Lobell DB, Schlenker W, Costa-Roberts J** (2011) Climate trends and global crop production
945 since 1980. *Science* **333**: 616–620
- 946 **Lopes CT, Franz M, Kazi F, Donaldson SL, Morris Q, Bader GD** (2010) Cytoscape Web: an
947 interactive web-based network browser. *Bioinformatics* **26**: 2347–2348
- 948 **Lynch J, Epstein E, Lauchli A, Weight GI** (1990) An automated greenhouse sand culture
949 system suitable for studies of P nutrition. *Plant Cell Environ* **13**: 547–554
- 950 **Lynch JP** (2013) Steep, cheap and deep: an ideotype to optimize water and N acquisition by
951 maize root systems. *Ann Bot* **112**: 347–357
- 952 **Lynch JP** (2019) Root phenotypes for improved nutrient capture: an underexploited opportunity
953 for global agriculture. *New Phytol* **223**: 548–564
- 954 **Lynch JP** (2018) Rightsizing root phenotypes for drought resistance. *J Exp Bot* **69**: 3279–3292
- 955 **Lynch JP, Chimungu JG, Brown KM** (2014) Root anatomical phenes associated with water
956 acquisition from drying soil: targets for crop improvement. *J Exp Bot* **65**: 6155–6166
- 957 **Mansueto L, Fuentes RR, Borja FN, Detras J, Abriol-Santos JM, Chebotarov D,**
958 **Sanciango M, Palis K, Copetti D, Poliakov A, et al** (2017) Rice SNP-seek database
959 update: new SNPs, indels, and queries. *Nucleic Acids Res* **45**: D1075–D1081
- 960 **Maurel C, Nacry P** (2020) Root architecture and hydraulics converge for acclimation to
961 changing water availability. *Nat Plants* **6**: 744–749
- 962 **Mazaheri M, Heckwolf M, Vaillancourt B, Gage JL, Burdo B, Heckwolf S, Barry K,**

- 963 **Lipzen A, Ribeiro CB, Kono TJY, et al** (2019) Genome-wide association analysis of stalk
964 biomass and anatomical traits in maize. *BMC Plant Biology* **19**: 1–17
- 965 **McCouch SR, Wright MH, Tung C-W, Maron LG, McNally KL, Fitzgerald M, Singh N,**
966 **DeClerck G, Agosto-Perez F, Korniliev P, et al** (2016) Open access resources for genome-
967 wide association mapping in rice. *Nat Commun* **7**: 10532
- 968 **McDermott JE, Taylor RC, Yoon H, Heffron F** (2009) Bottlenecks and hubs in inferred
969 networks are important for virulence in *Salmonella typhimurium*. *J Comput Biol* **16**: 169–
970 180
- 971 **McLaren W, Gil L, Hunt SE, Riat HS, Ritchie GRS, Thormann A, Flicek P, Cunningham**
972 **F** (2016) The Ensembl Variant Effect Predictor. *Genome Biol* **17**: 1–14
- 973 **Milhinhos A, Miguel CM** (2013) Hormone interactions in xylem development: a matter of
974 signals. *Plant Cell Reports* **32**: 867–883
- 975 **Okekeogbu IO, Pattathil S, González Fernández-Niño SM, Aryal UK, Penning BW, Lao J,**
976 **Heazlewood JL, Hahn MG, McCann MC, Carpita NC** (2019) Glycome and Proteome
977 Components of Golgi Membranes Are Common between Two Angiosperms with Distinct
978 Cell-Wall Structures. *Plant Cell* **31**: 1094–1112
- 979 **Oyiga BC, Palczak J, Wojciechowski T, Lynch JP, Naz AA, Léon J, Ballvora A** (2020)
980 Genetic components of root architecture and anatomy adjustments to water-deficit stress in
981 spring barley. *Plant Cell Environ* **43**: 692–711
- 982 **Parent B, Hachez C, Redondo E, Simonneau T, Chaumont F, Tardieu F** (2009) Drought and
983 abscisic acid effects on aquaporin content translate into changes in hydraulic conductivity
984 and leaf growth rate: a trans-scale approach. *Plant Physiol* **149**: 2000–2012
- 985 **Pesquet E, Tuominen H** (2011) Ethylene stimulates tracheary element differentiation in *Zinnia*
986 *elegans* cell cultures. *New Phytol* **190**: 138–149
- 987 **Pires MV, de Castro EM, de Freitas BSM, Souza Lira JM, Magalhães PC, Pereira MP**
988 (2020) Yield-related phenotypic traits of drought resistant maize genotypes. *Environ Exp*
989 *Bot* **171**: 1–10
- 990 **Portwood JL, Woodhouse MR, Cannon EK, Gardiner JM, Harper LC, Schaeffer ML,**
991 **Walsh JR, Sen TZ, Cho KT, Schott DA, et al** (2018) MaizeGDB 2018: the maize multi-
992 genome genetics and genomics database. *Nucleic Acids Research* **47**: 1146–1154
- 993 **Purushothaman R, Zaman-Allah M, Mallikarjuna N, Pannirselvam R, Krishnamurthy L,**
994 **Gowda CLL** (2013) Root Anatomical Traits and Their Possible Contribution to Drought
995 Tolerance in Grain Legumes. *Plant Prod Sci* **16**: 1–8
- 996 **Qin L-X, Li Y, Li D-D, Xu W-L, Zheng Y, Li X-B** (2014) Arabidopsis drought-induced
997 protein Di19-3 participates in plant response to drought and high salinity stresses. *Plant Mol*
998 *Biol* **86**: 609–625

- 999 **Ramachandran P, Augstein F, Nguyen V, Carlsbecker A** (2020) Coping With Water
1000 Limitation: Hormones That Modify Plant Root Xylem Development. *Front Plant Sci* **11**: 570
- 1001 **Ramachandran P, Wang G, Augstein F, de Vries J, Carlsbecker A** (2018) Continuous root
1002 xylem formation and vascular acclimation to water deficit involves endodermal ABA
1003 signalling via miR165. *Development* **145**: 1-7
- 1004 **R Core Team** (2020) R: A language and environment for statistical computing. R Foundation
1005 for Statistical Computing, Vienna, Austria
- 1006 **Richards RA, Passioura JB** (1989) A breeding program to reduce the diameter of the major
1007 xylem vessel in the seminal roots of wheat and its effect on grain-yield in rain-fed
1008 environments. *Aust J Agric Res* **40**: 943–950
- 1009 **Richmond TA, Somerville CR** (2000) The cellulose synthase superfamily. *Plant Physiol* **124**:
1010 495–498
- 1011 **Roberts K, McCann MC** (2000) Xylogenesis: the birth of a corpse. *Curr Opin Plant Biol* **3**:
1012 517–522
- 1013 **Růžička K, Ursache R, Hejátko J, Helariutta Y** (2015) Xylem development - from the cradle
1014 to the grave. *New Phytol* **207**: 519–535
- 1015 **Salse J, Piegu B, Cooke R, Delseny M** (2004) New in silico insight into the synteny between
1016 rice (*Oryza sativa* L.) and maize (*Zea mays* L.) highlights reshuffling and identifies new
1017 duplications in the rice genome. *The Plant Journal* **38**: 396–409
- 1018 **Schaefer RJ, Michno J-M, Jeffers J, Hoekenga O, Dilkes B, Baxter I, Myers CL** (2018)
1019 Integrating Coexpression Networks with GWAS to Prioritize Causal Genes in Maize. *Plant*
1020 *Cell* **30**: 2922–2942
- 1021 **Schaefer RJ, Michno J-M, Myers CL** (2017) Unraveling gene function in agricultural species
1022 using gene co-expression networks. *Biochim Biophys Acta Gene Regul Mech* **1860**: 53–63
- 1023 **Schnable PS, Ware D, Fulton RS, Stein JC, Wei F, Pasternak S, Liang C, Zhang J, Fulton**
1024 **L, Graves TA, et al** (2009) The B73 Maize Genome: Complexity, Diversity, and Dynamics.
1025 *Science* **326**: 1112–1115
- 1026 **Schneider HM, Klein SP, Hanlon MT, Kaeppler S, Brown KM, Lynch JP** (2020a) Genetic
1027 control of root anatomical plasticity in maize. *Plant Genome* **13**: 1–14
- 1028 **Schneider HM, Klein SP, Hanlon MT, Nord EA, Kaeppler S, Brown KM, Warry A,**
1029 **Bhosale R, Lynch JP** (2020b) Genetic Control of Root Architectural Plasticity in Maize. *J*
1030 *Exp Bot* **71**: 3185–3197
- 1031 **Schneider HM, Lynch JP** (2020) Should Root Plasticity Be a Crop Breeding Target? *Front*
1032 *Plant Sci* **11**: 1–16
- 1033 **Schuetz M, Smith R, Ellis B** (2012) Xylem tissue specification, patterning, and differentiation

- 1034 mechanisms. *J Exp Bot* **64**: 11–31
- 1035 **Smith BG, Harris PJ** (1999) The polysaccharide composition of Poales cell walls: Poaceae cell
1036 walls are not unique. *Biochem Syst Ecol* **27**: 33–53
- 1037 **Sosa JM, Huber DE, Welk B, Fraser HL** (2014) Development and application of MIPARTM: a
1038 novel software package for two- and three-dimensional microstructural characterization.
1039 *Integrating Materials and Manufacturing Innovation* **3**: 123–140
- 1040 **de Souza TC, de Castro EM, César Magalhães P, De Oliveira Lino L, Trindade Alves E, de**
1041 **Albuquerque PEP** (2013) Morphophysiology, morphoanatomy, and grain yield under field
1042 conditions for two maize hybrids with contrasting response to drought stress. *Acta Physiol*
1043 *Plant* **35**: 3201–3211
- 1044 **Sperry JS, Saliendra NZ** (1994) Intra- and inter-plant variation in xylem cavitation in *Betula*
1045 *occidentalis*. *Plant Cell Environ* **17**: 1233–1241
- 1046 **Stelpflug SC, Sekhon RS, Vaillancourt B, Hirsch CN, Buell CR, de Leon N, Kaeppler SM**
1047 (2016) An Expanded Maize Gene Expression Atlas based on RNA Sequencing and its Use
1048 to Explore Root Development. *Plant Genome* **9**: 1–16
- 1049 **Stöver BC, Müller KF** (2010) TreeGraph 2: Combining and visualizing evidence from different
1050 phylogenetic analyses. *BMC Bioinformatics* **11**: 1–9
- 1051 **Strock CF, Schneider HM, Galindo-Castañeda T, Hall BT, Van Gansbeke B, Mather DE,**
1052 **Roth MG, Chilvers MI, Guo X, Brown K, et al** (2019) Laser ablation tomography for
1053 visualization of root colonization by edaphic organisms. *Journal of Experimental Botany* **70**:
1054 5327–5342
- 1055 **Szekeres M, Németh K, Koncz-Kálmán Z, Mathur J, Kauschmann A, Altmann T, Rédei**
1056 **GP, Nagy F, Schell J, Koncz C** (1996) Brassinosteroids rescue the deficiency of CYP90, a
1057 cytochrome P450, controlling cell elongation and de-etiolation in *Arabidopsis*. *Cell* **85**: 171–
1058 182
- 1059 **Taylor NG, Howells RM, Huttly AK, Vickers K, Turner SR** (2003) Interactions among three
1060 distinct CesaA proteins essential for cellulose synthesis. *Proc Natl Acad Sci U S A* **100**:
1061 1450–1455
- 1062 **Trachsel S, Kaeppler SM, Brown KM, Lynch JP** (2010) Shovelomics: high throughput
1063 phenotyping of maize (*Zea mays* L.) root architecture in the field. *Plant Soil* **341**: 75–87
- 1064 **Turco GM, Rodriguez-Medina J, Siebert S, Han D, Valderrama-Gómez MÁ, Vahldick H,**
1065 **Shulse CN, Cole BJ, Juliano CE, Dickel DE, et al** (2019) Molecular Mechanisms Driving
1066 Switch Behavior in Xylem Cell Differentiation. *Cell Rep* **28**: 342–351.e4
- 1067 **Uga Y, Sugimoto K, Ogawa S, Rane J, Ishitani M, Hara N, Kitomi Y, Inukai Y, Ono K,**
1068 **Kanno N, et al** (2013) Control of root system architecture by DEEPER ROOTING 1
1069 increases rice yield under drought conditions. *Nat Genet* **45**: 1097–1102

- 1070 **Vadez V** (2014) Root hydraulics: The forgotten side of roots in drought adaptation. *Field Crops*
1071 *Res* **165**: 15–24
- 1072 **Vadez V, Kholova J, Medina S, Kakkera A, Anderberg H** (2014) Transpiration efficiency:
1073 new insights into an old story. *J Exp Bot* **65**: 6141–6153
- 1074 **Vejchasarn P** (2014) Nutritional and Genetic Architecture of Root Traits in Rice (*Oryza sativa*).
1075 Ph.D. The Pennsylvania State University.
- 1076 **Vilagrosa A, Chirino E, Peguero-Pina JJ, Barigah TS, Cochard H, Gil-Pelegrín E** (2012)
1077 Xylem Cavitation and Embolism in Plants Living in Water-Limited Ecosystems. *In* R
1078 Aroca, ed, *Plant Responses to Drought*. Springer-Verlag, pp 63–109
- 1079 **Vogel J** (2008) Unique aspects of the grass cell wall. *Curr Opin Plant Biol* **11**: 301–307
- 1080 **Wahl S, Ryser P** (2000) Root tissue structure is linked to ecological strategies of grasses. *New*
1081 *Phytol* **148**: 459–471
- 1082 **Wang DR, Agosto-Pérez FJ, Chebotarov D, Shi Y, Marchini J, Fitzgerald M, McNally KL,**
1083 **Alexandrov N, McCouch SR** (2018) An imputation platform to enhance integration of rice
1084 genetic resources. *Nat Commun* **9**: 3519
- 1085 **Wasson AP, Richards RA, Chatrath R, Misra SC, Prasad SVS, Rebetzke GJ, Kirkegaard**
1086 **JA, Christopher J, Watt M** (2012) Traits and selection strategies to improve root systems
1087 and water uptake in water-limited wheat crops. *J Exp Bot* **63**: 3485–3498
- 1088 **Wickham H** (2016) *ggplot2: Elegant Graphics for Data Analysis*. Springer-Verlag, New York
- 1089 **Yamaguchi M, Goué N, Igarashi H, Ohtani M, Nakano Y, Mortimer JC, Nishikubo N,**
1090 **Kubo M, Katayama Y, Kakegawa K, et al** (2010a) VASCULAR-RELATED NAC-
1091 DOMAIN6 and VASCULAR-RELATED NAC-DOMAIN7 effectively induce
1092 transdifferentiation into xylem vessel elements under control of an induction system. *Plant*
1093 *Physiol* **153**: 906–914
- 1094 **Yamaguchi M, Mitsuda N, Ohtani M, Ohme-Takagi M, Kato K, Demura T** (2011)
1095 VASCULAR-RELATED NAC-DOMAIN 7 directly regulates the expression of a broad
1096 range of genes for xylem vessel formation: Direct target genes of VND7. *Plant J* **66**: 579–
1097 590
- 1098 **Yamaguchi M, Ohtani M, Mitsuda N, Kubo M, Ohme-Takagi M, Fukuda H, Demura T**
1099 (2010b) VND-INTERACTING2, a NAC domain transcription factor, negatively regulates
1100 xylem vessel formation in *Arabidopsis*. *Plant Cell* **22**: 1249–1263
- 1101 **Yoshida S, Forno DA, Bhadrachalam A** (1971) Zinc deficiency of the rice plant on calcareous
1102 and neutral soils in the philippines. *Soil Sci Plant Nutr* **17**: 83–87
- 1103 **Yu H, Greenbaum D, Xin Lu H, Zhu X, Gerstein M** (2004) Genomic analysis of essentiality
1104 within protein networks. *Trends Genet* **20**: 227–231

- 1105 **Yu H, Kim PM, Sprecher E, Trifonov V, Gerstein M** (2007) The importance of bottlenecks in
1106 protein networks: correlation with gene essentiality and expression dynamics. *PLoS Comput*
1107 *Biol* **3**: e59
- 1108 **Zaman-Allah M, Jenkinson DM, Vadez V** (2011) A conservative pattern of water use, rather
1109 than deep or profuse rooting, is critical for the terminal drought tolerance of chickpea. *J Exp*
1110 *Bot* **62**: 4239–4252
- 1111 **Zhan A, Schneider H, Lynch JP** (2015) Reduced Lateral Root Branching Density Improves
1112 Drought Tolerance in Maize. *Plant Physiol* **168**: 1603–1615
- 1113 **Zhang X, Pang J, Ma X, Zhang Z, He Y, Hirsch CN, Zhao J** (2019) Multivariate analyses of
1114 root phenotype and dynamic transcriptome underscore valuable root traits and water-deficit
1115 responsive gene networks in maize. *Plant Direct* **3**: 1–18
- 1116 **Zhao K, Tung C-W, Eizenga GC, Wright MH, Ali ML, Price AH, Norton GJ, Islam MR,**
1117 **Reynolds A, Mezey J, et al** (2011) Genome-wide association mapping reveals a rich
1118 genetic architecture of complex traits in *Oryza sativa*. *Nat Commun* **2**: 467
- 1119 **Zheng Z, Hey S, Jubery T, Liu H, Yang Y, Coffey L, Miao C, Sigmon B, Schnable JC,**
1120 **Hochholdinger F, et al** (2020) Shared Genetic Control of Root System Architecture
1121 between *Zea mays* and *Sorghum bicolor*. *Plant Physiol* **182**: 977–991
- 1122 **Zhu J, Brown KM, Lynch JP** (2010) Root cortical aerenchyma improves the drought tolerance
1123 of maize (*Zea mays* L.). *Plant Cell Environ* **9**: 31
- 1124

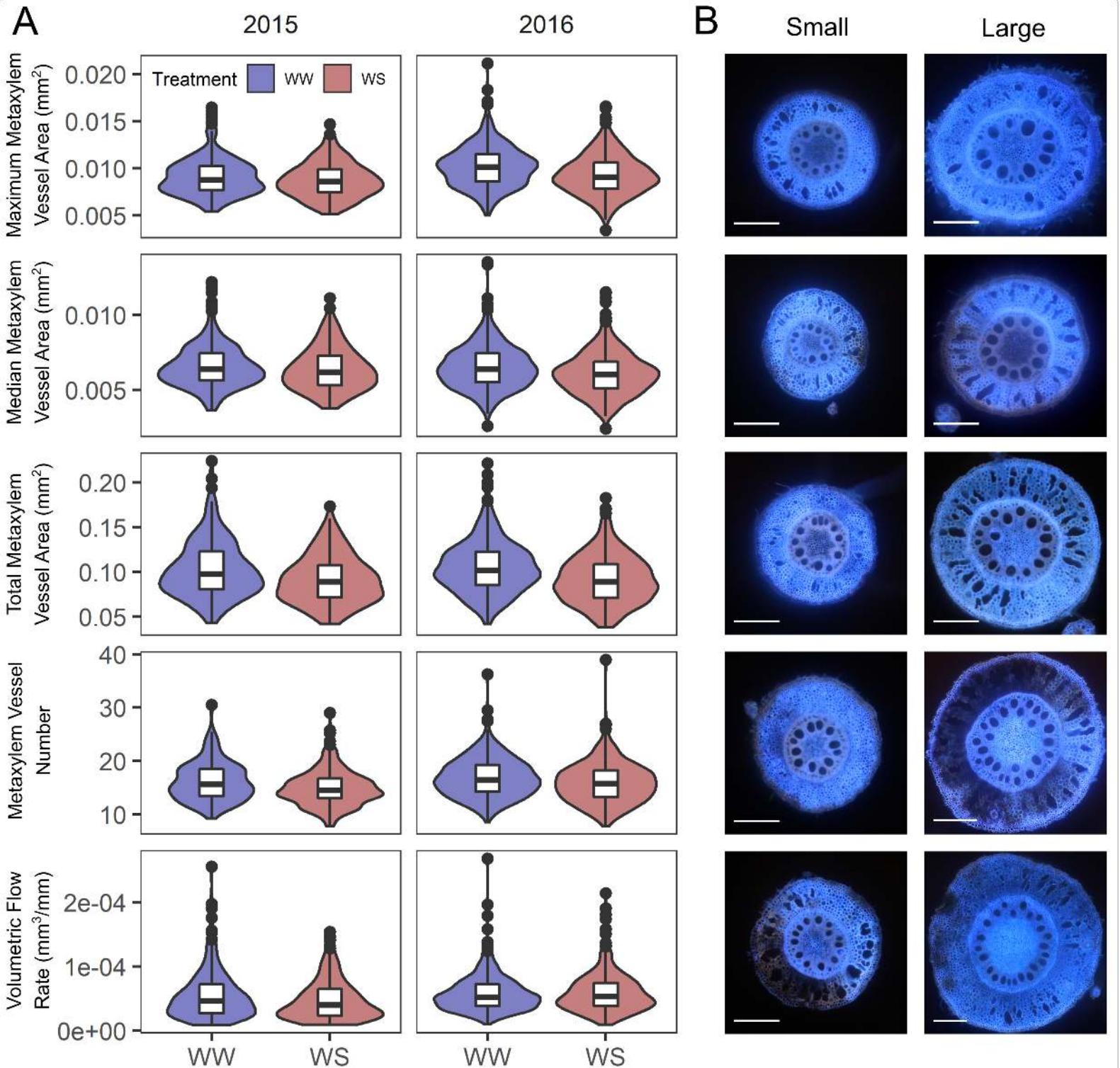


Figure 1. Wide variation exists in metaxylem phenes under well-watered and water stress conditions in the field. (A) Violin plots show the distribution of each metaxylem phene under well-watered (WW, blue) and water stress (WS, red) in each field season while the overlaid box plots show the median bounded by the first and third quartile. Two-way ANOVA determined statistical differences between treatments and growth seasons (Table 1). (B) Root cross-sectional images collected via laser ablation tomography illustrate the range in each metaxylem phenotype. White scale bars in the bottom left of each image are equal to 0.5 mm.

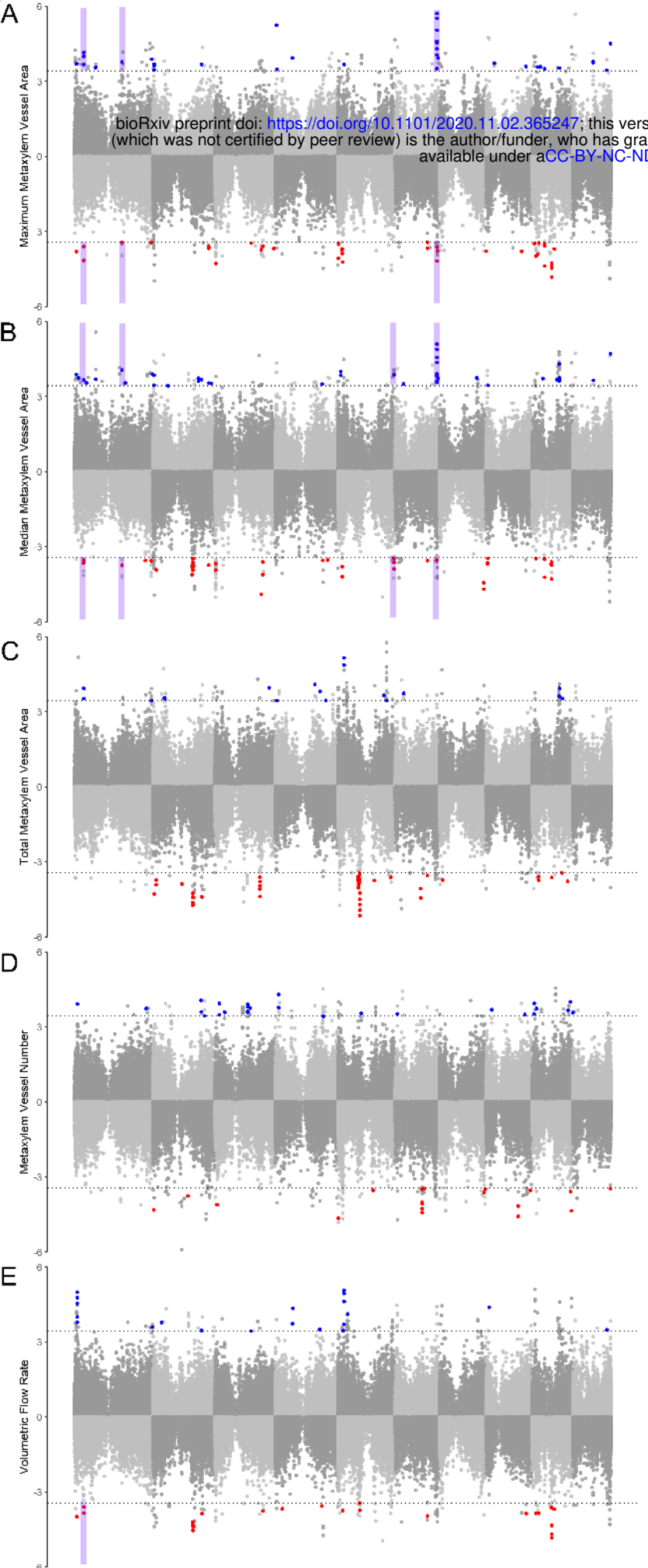


Figure 2. Manhattan plots of the results of the GWAS for (A) maximum metaxylem vessel area, (B) median metaxylem vessel area, (C) total metaxylem vessel area, (D) metaxylem vessel number and (E) volumetric flow rate in each watering regime in 2016 (grey). Results from the well-watered studies are shown on the positive axis while the water stress is on the negative axis. The dotted line indicates the significance threshold ($-\log_{10}(p\text{-value}) > 3.43$). Dots colored blue and red are significant SNPs with consistent allelic effects in the 2015 GWAS in the well-watered and water-stressed treatments, respectively. Select genomic regions that shared significant SNPs in both treatments have been highlighted in purple.

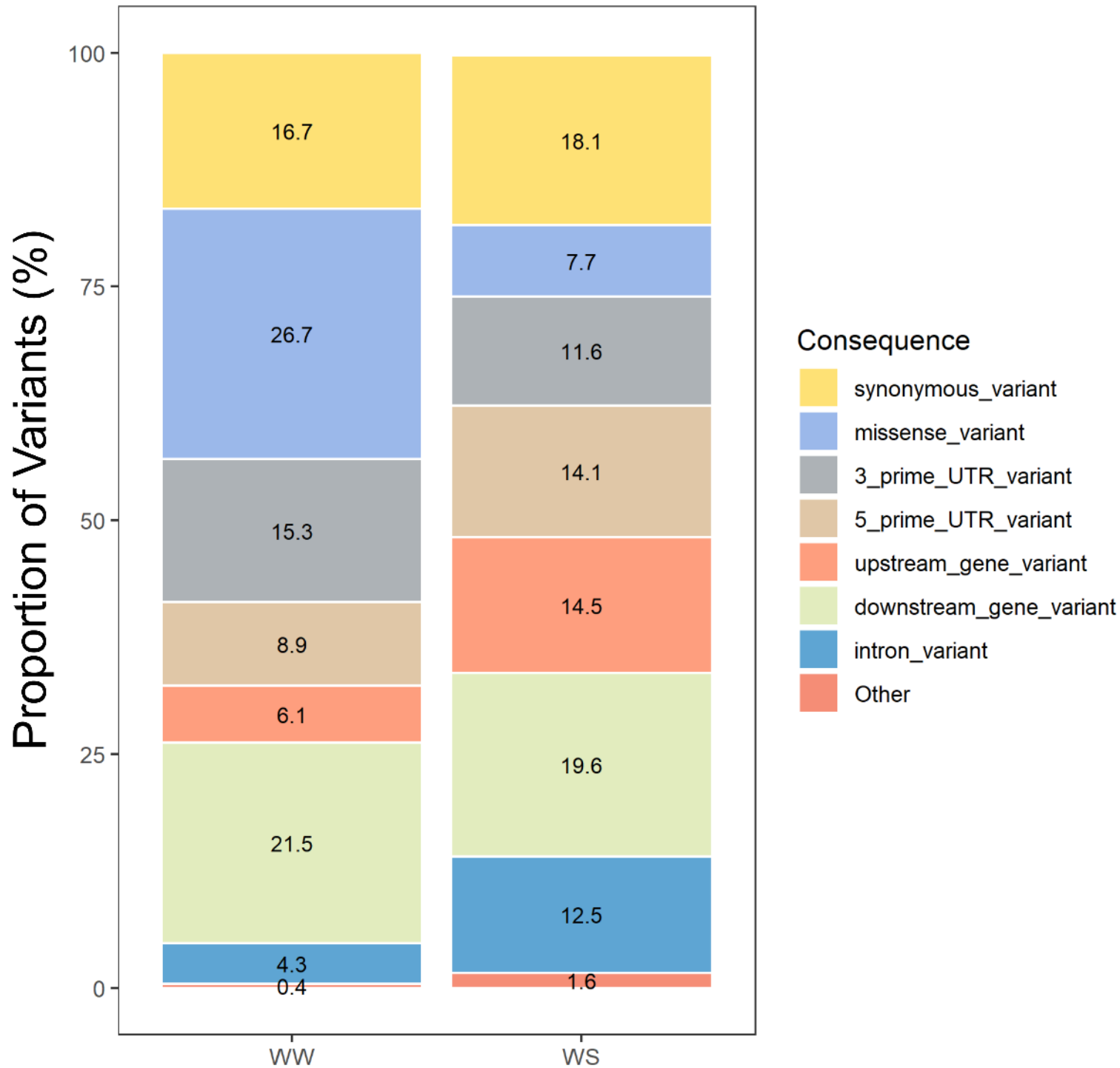
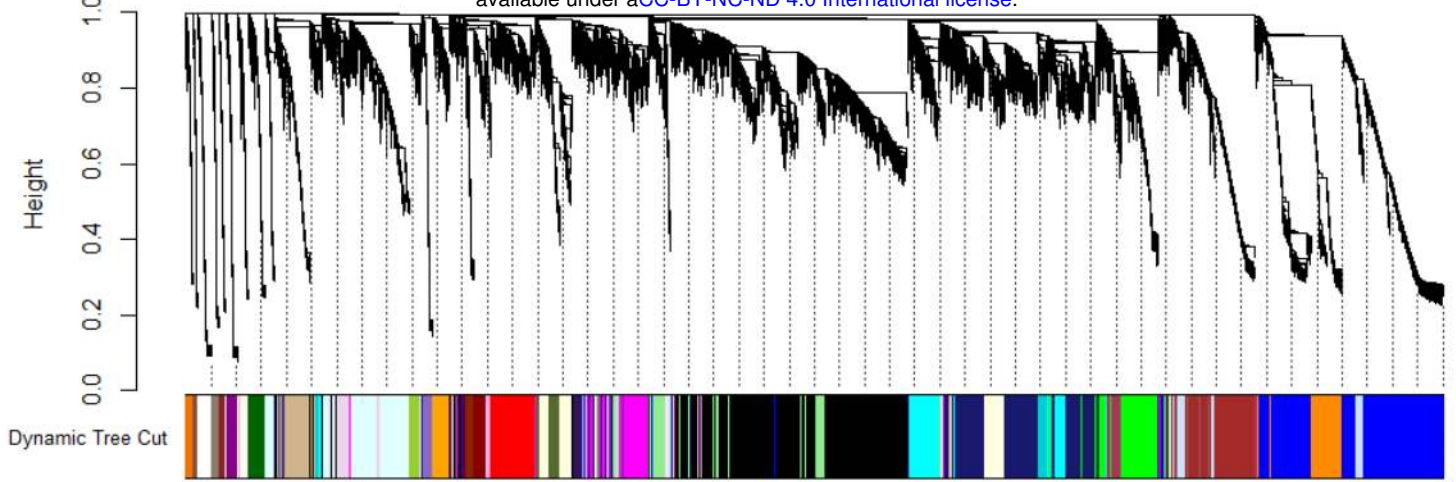
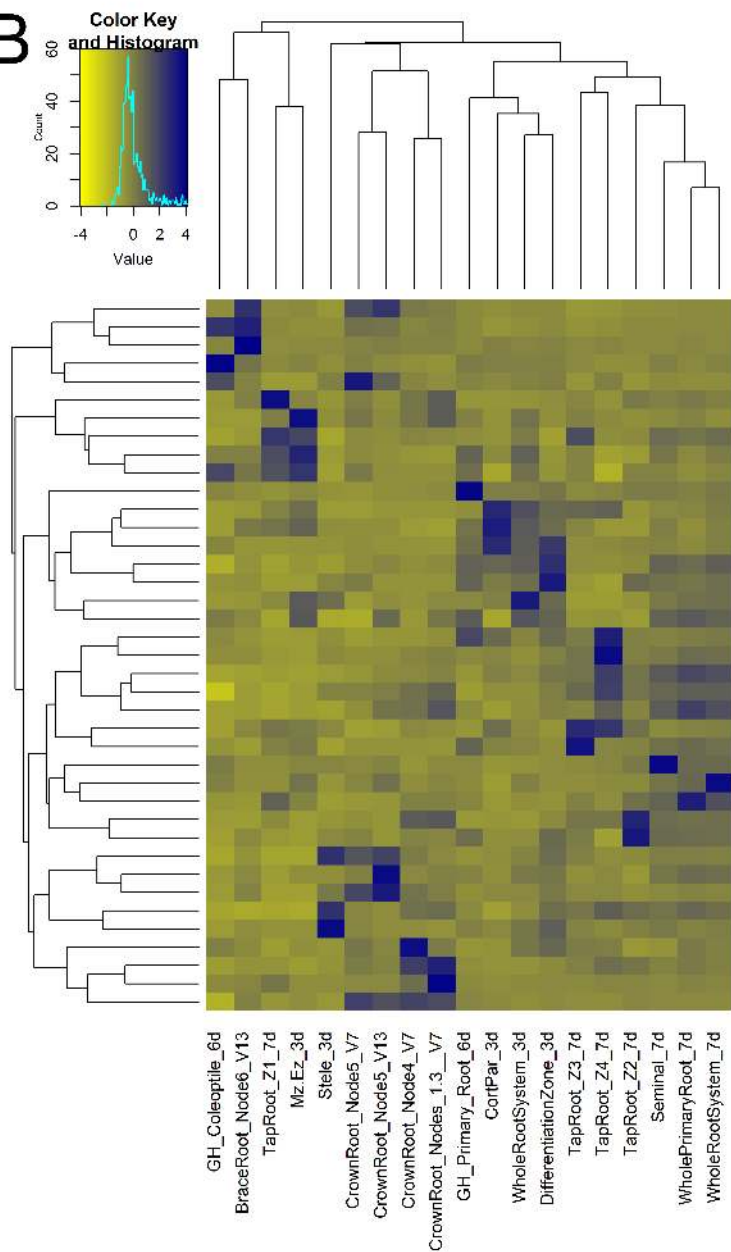


Figure 3. Predicted consequences of minor allele variants presented as a proportion of the total number of significant SNPs in well-watered (WW) and water stressed (WS) conditions.

A



B



C

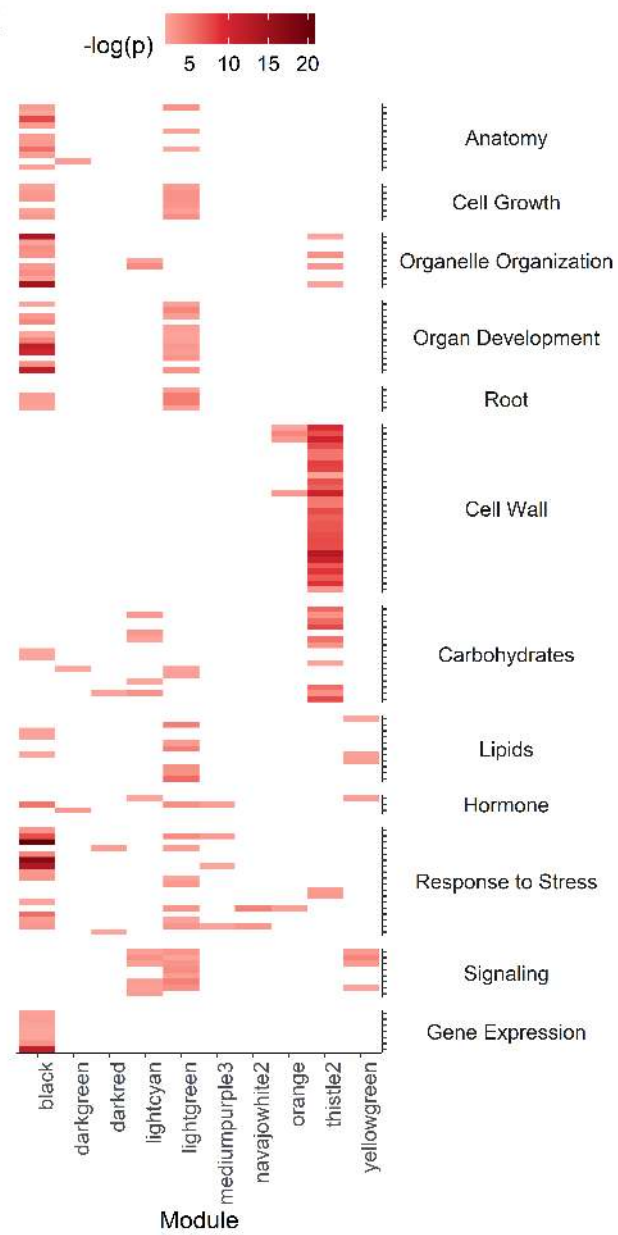


Figure 4. A gene co-expression network and significant correlation of modules. (A) Hierarchical clustering dendrogram displaying 39 modules of co-expressed genes. (B) A heatmap showing the significance of the correlation ($\log(p)$ -value) between modules and various root tissues. (C) Inferred biological function of modules most likely associated metaxylem development based on GO analysis. Only GO terms most relevant to xylem development are displayed. No GO terms were over-represented by modules “lightcyan1”, “salmon4”, and “thistle1”.

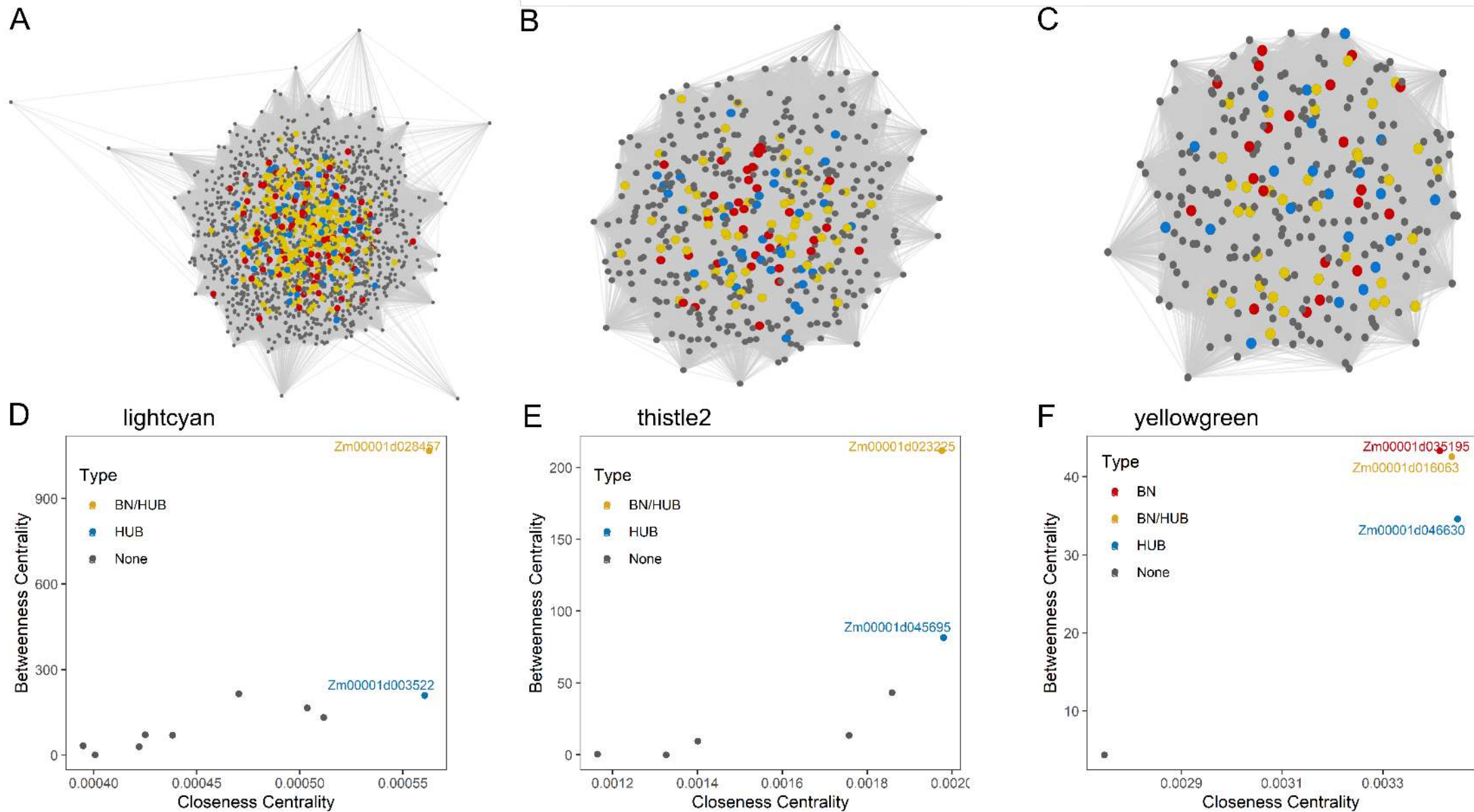


Figure 5. Gene co-expression subnetworks for modules associated with root stele 3 days after sowing. These modules were “lightcyan” (A, D), “thistle2” (B, E) and “yellowgreen” (C, F). Network visualizations (A, B, C) show all interactions within the subnetwork. Scatterplots (D, E, F) show the calculated closeness centrality and betweenness centrality for candidate genes determined by GWAS residing in the corresponding module. All bottleneck (BN), bottleneck/hub (BN/HUB) and hub (HUB) genes are shown in red, yellow, and blue, respectively.

A Maize WS Maize WW

118 6 114

bioRxiv preprint doi: <https://doi.org/10.1101/2020.11.02.365247>; this version posted November 4, 2020. The copyright holder for this preprint (which was not certified by peer review) is the author/funder, who has granted bioRxiv a license to display the preprint in perpetuity. It is made available under aCC-BY-NC-ND 4.0 International license.

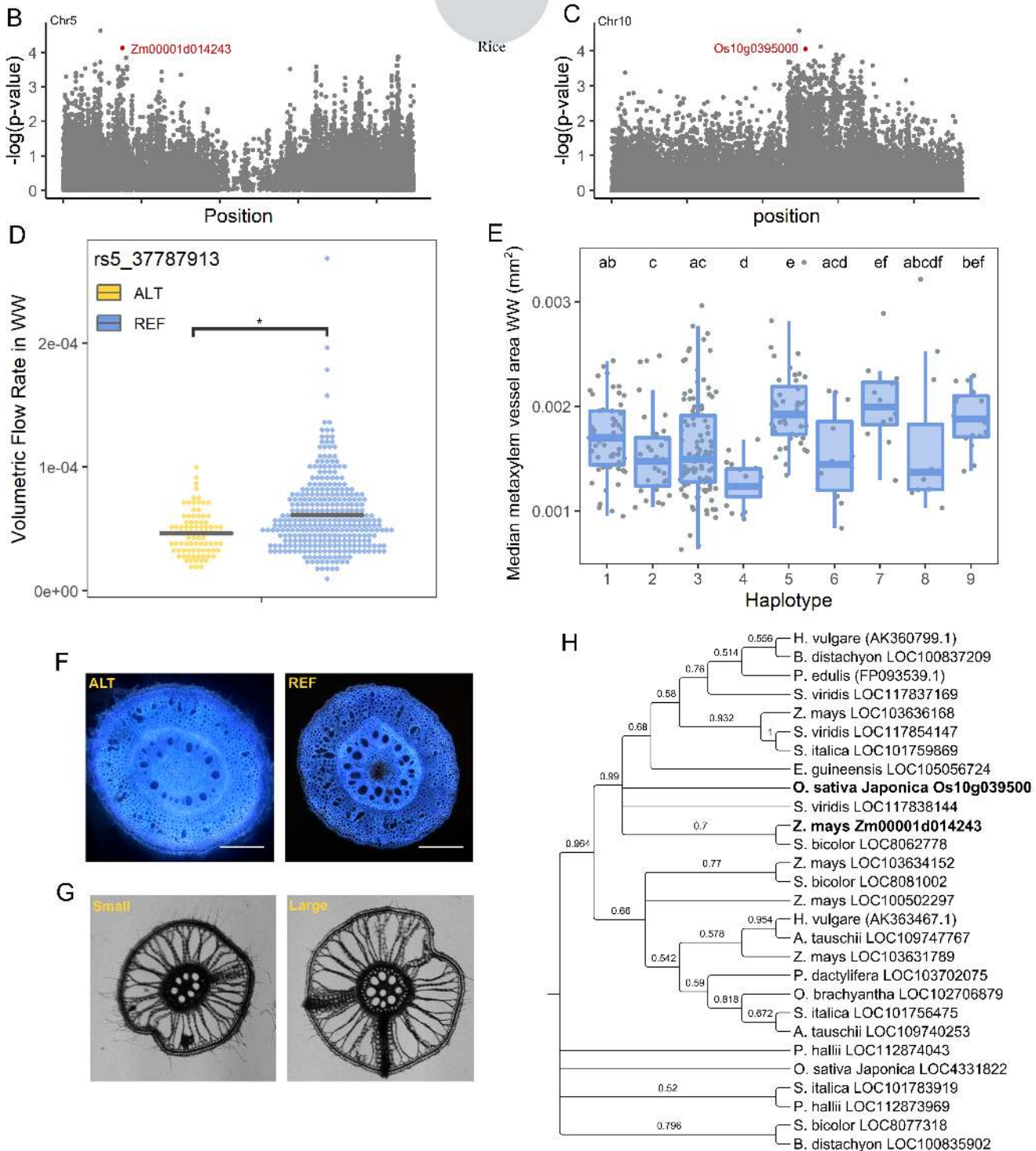


Figure 6. Comparative GWAS between maize and rice for metaxylem phenes identified a syntenic gene pair encoding root-specific kinase 1 associated with root metaxylem phenotypes. (A) Comparison of the results of three GWAS seeking genetic loci associated with root metaxylem phenes in maize under well-watered (WW) and water-stressed (WS) conditions and rice. (B) Manhattan plot of SNPs and their associated with the volumetric flow rate under WW on maize chromosome 5 highlighting the candidate gene (Zm00001d014243) in red. (C) Manhattan plot of SNPs associated with metaxylem vessel area on rice chromosome 10 highlighting the candidate gene (Os10g0395000) in red. (D) Significant differences in volumetric flow rate in WW are associated with the minor allele (ALT, yellow) compared to the major allele (REF, blue) determined by two-sample t-test ($p < 0.001$). (E) Significant differences in metaxylem vessel area are associated with nine haplotypes of Os10g0395000 determined by Kruskal-Wallis ($p < 0.001$). Haplotypes are disclosed in Supplemental Figure S6. (F) Representative images maize root cross-sections captured via LAT illustrating visual phenotypic differences in individuals that contained the minor (ALT) and major (REF) alleles. (G) Representative images of rice root cross-sections collected by hand-sectioning illustrating visual contrasts in metaxylem vessel area. (H) Phylogenetic tree of gene homologous to root-specific kinase 1. The amino acid sequences of 28 proteins of high sequence similarity were aligned by MUSCLE and the phylogenetic tree was constructed using MEGA version 10.1.8 and TreeGraph 2. Bootstrap values from 500 replicates were used to assess the robustness of the tree. The maize and rice candidate genes identified in GWAS are labeled in bold.

Parsed Citations

- Abd Allah AA, Badawy SA, Zayed BA, El. Gohary AA (2010) The Role of Root System Traits in the Drought Tolerance of Rice (*Oryza sativa* L.). International Journal of Agricultural and Biological Sciences 1: 83–87**
Google Scholar: [Author Only](#) [Title Only](#) [Author and Title](#)
- Alves MS, Reis PAB, Dadalto SP, Faria JAQA, Fontes EPB, Fietto LG (2011) A novel transcription factor, ERD15 (Early Responsive to Dehydration 15), connects endoplasmic reticulum stress with an osmotic stress-induced cell death signal. J Biol Chem 286: 20020–20030**
Google Scholar: [Author Only](#) [Title Only](#) [Author and Title](#)
- Balestrazzi A, Confalonieri M, Macovei A, Donà M, Carbonera D (2011) Genotoxic stress and DNA repair in plants: emerging functions and tools for improving crop productivity. Plant Cell Rep 30: 287–295**
Google Scholar: [Author Only](#) [Title Only](#) [Author and Title](#)
- Bekh-Ochir D, Shimada S, Yamagami A, Kanda S, Ogawa K, Nakazawa M, Matsui M, Sakuta M, Osada H, Asami T, et al (2013) A novel mitochondrial DnaJ/Hsp40 family protein BIL2 promotes plant growth and resistance against environmental stress in brassinosteroid signaling. Planta 237: 1509–1525**
Google Scholar: [Author Only](#) [Title Only](#) [Author and Title](#)
- Bennetzen JL, Freeling M (1997) The unified grass genome: synergy in synteny. Genome Res 7: 301–306**
Google Scholar: [Author Only](#) [Title Only](#) [Author and Title](#)
- Berker R (1963) Intégration des équations du mouvement d'un fluide visqueux incompressible. Handbuch der Physik 3: 1–384**
Google Scholar: [Author Only](#) [Title Only](#) [Author and Title](#)
- Buell CR, Yuan Q, Ouyang S, Liu J, Zhu W, Wang A, Maiti R, Haas B, Wortman J, Pertea M, et al (2005) Sequence, annotation, and analysis of synteny between rice chromosome 3 and diverged grass species. Genome Res 15: 1284–1291**
Google Scholar: [Author Only](#) [Title Only](#) [Author and Title](#)
- Burrige JD, Rangarajan H, Lynch JP (2020) Comparative phenomics of annual grain legume root architecture. Crop Sci 1–20**
Google Scholar: [Author Only](#) [Title Only](#) [Author and Title](#)
- Burton AL, Williams M, Lynch JP, Brown KM (2012) RootScan: Software for high-throughput analysis of root anatomical traits. Plant Soil 357: 189–203**
Google Scholar: [Author Only](#) [Title Only](#) [Author and Title](#)
- Carpita NC (1996) Structure and biogenesis of the cell walls of grasses. Annual Reviews in Plant Physiology Plant Molecular Biology 47: 445–476**
Google Scholar: [Author Only](#) [Title Only](#) [Author and Title](#)
- Chang CC, Chow CC, Tellier LC, Vattikuti S, Purcell SM, Lee JJ (2015) Second-generation PLINK: rising to the challenge of larger and richer datasets. Gigascience 4: 1–16**
Google Scholar: [Author Only](#) [Title Only](#) [Author and Title](#)
- Chen W, Wang W, Peng M, Gong L, Gao Y, Wan J, Wang S, Shi L, Zhou B, Li Z, et al (2016) Comparative and parallel genome-wide association studies for metabolic and agronomic traits in cereals. Nature Communications 7: 1–10**
Google Scholar: [Author Only](#) [Title Only](#) [Author and Title](#)
- Chimungu JG, Brown KM, Lynch JP (2014a) Large root cortical cell size improves drought tolerance in maize. Plant Physiol 166: 2166–2178**
Google Scholar: [Author Only](#) [Title Only](#) [Author and Title](#)
- Chimungu JG, Brown KM, Lynch JP (2014b) Reduced root cortical cell file number improves drought tolerance in maize. Plant Physiol 166: 1943–1955**
Google Scholar: [Author Only](#) [Title Only](#) [Author and Title](#)
- Choe S, Dilkes BP, Gregory BD, Ross AS, Yuan H, Noguchi T, Fujioka S, Takatsuto S, Tanaka A, Yoshida S, et al (1999a) The Arabidopsis dwarf1 mutant is defective in the conversion of 24-methylenecholesterol to campesterol in brassinosteroid biosynthesis. Plant Physiol 119: 897–907**
Google Scholar: [Author Only](#) [Title Only](#) [Author and Title](#)
- Choe S, Noguchi T, Fujioka S, Takatsuto S, Tissier CP, Gregory BD, Ross AS, Tanaka A, Yoshida S, Tax FE, et al (1999b) The Arabidopsis dwf7/ste1 mutant is defective in the delta7 sterol C-5 desaturation step leading to brassinosteroid biosynthesis. Plant Cell 11: 207–221**
Google Scholar: [Author Only](#) [Title Only](#) [Author and Title](#)
- Comas LH, Becker SR, Cruz VMV, Byrne PF, Dierig DA (2013) Root traits contributing to plant productivity under drought. Front Plant Sci 4: 1–16**
Google Scholar: [Author Only](#) [Title Only](#) [Author and Title](#)
- Csardi G, Nepusz T (2006) The igraph software package for complex network research. InterJournal, Complex Systems 1695**
Google Scholar: [Author Only](#) [Title Only](#) [Author and Title](#)

Dai A (2013) Increasing drought under global warming in observations and models. *Nat Clim Chang* 3: 52–58

Google Scholar: [Author Only](#) [Title Only](#) [Author and Title](#)

Daryanto S, Wang L, Jacinthe P-A (2016) Global Synthesis of Drought Effects on Maize and Wheat Production. *PLoS One* 11: e0156362

Google Scholar: [Author Only](#) [Title Only](#) [Author and Title](#)

Denancé N, Szurek B, Noël LD (2014) Emerging functions of nodulin-like proteins in non-nodulating plant species. *Plant Cell Physiol* 55: 469–474

Google Scholar: [Author Only](#) [Title Only](#) [Author and Title](#)

Du Z, Zhou X, Ling Y, Zhang Z, Su Z (2010) agriGO: a GO analysis toolkit for the agricultural community. *Nucleic Acids Res* 38: W64–70

Google Scholar: [Author Only](#) [Title Only](#) [Author and Title](#)

Endelman JB (2011) Ridge regression and other kernels for genomic selection with R package rrBLUP. *Plant Genome* 4: 250–255

Google Scholar: [Author Only](#) [Title Only](#) [Author and Title](#)

Fehr W (1991) Principles of Cultivar Development: Theory and Technique. Iowa State University

Google Scholar: [Author Only](#) [Title Only](#) [Author and Title](#)

Feng W, Lindner H, Robbins NE 2nd, Dinneny JR (2016) Growing Out of Stress: The Role of Cell- and Organ-Scale Growth Control in Plant Water-Stress Responses. *Plant Cell* 28: 1769–1782

Google Scholar: [Author Only](#) [Title Only](#) [Author and Title](#)

Finkelstein R (2013) Abscisic Acid synthesis and response. In C Somerville, E Meyerowitz, eds, *The Arabidopsis Book*. pp 1–36

Google Scholar: [Author Only](#) [Title Only](#) [Author and Title](#)

Gao Y, Lynch JP (2016) Reduced crown root number improves water acquisition under water deficit stress in maize (*Zea mays* L.). *J Exp Bot* 67: 4545–4557

Google Scholar: [Author Only](#) [Title Only](#) [Author and Title](#)

Guet J, Fichot R, Lédée C, Laurans F, Cochard H, Delzon S, Bastien C, Brignolas F (2015) Stem xylem resistance to cavitation is related to xylem structure but not to growth and water-use efficiency at the within-population level in *Populus nigra* L. *J Exp Bot* 66: 4643–4652

Google Scholar: [Author Only](#) [Title Only](#) [Author and Title](#)

Guo H, Li L, Ye H, Yu X, Algreen A, Yin Y (2009a) Three related receptor-like kinases are required for optimal cell elongation in *Arabidopsis thaliana*. *Proc Natl Acad Sci U S A* 106: 7648–7653

Google Scholar: [Author Only](#) [Title Only](#) [Author and Title](#)

Guo H, Ye H, Li L, Yin Y (2009b) A family of receptor-like kinases are regulated by BES1 and involved in plant growth in *Arabidopsis thaliana*. *Plant Signal Behav* 4: 784–786

Google Scholar: [Author Only](#) [Title Only](#) [Author and Title](#)

Hacke UG, Sperry JS (2001) Functional and ecological xylem anatomy. *Perspect Plant Ecol Evol Syst* 4: 97–115

Google Scholar: [Author Only](#) [Title Only](#) [Author and Title](#)

Hall BG (2013) Building phylogenetic trees from molecular data with MEGA. *Mol Biol Evol* 30: 1229–1235

Google Scholar: [Author Only](#) [Title Only](#) [Author and Title](#)

Hall B, Lanba A, Lynch J (2019) Three-dimensional analysis of biological systems via a novel laser ablation technique. *J Laser Appl* 31: 022602

Google Scholar: [Author Only](#) [Title Only](#) [Author and Title](#)

Hansey CH, Johnson JM, Sekhon RS, Kaeppler SM, de Leon N (2011) Genetic diversity of a maize association population with restricted phenology. *Crop Sci* 51: 704–715

Google Scholar: [Author Only](#) [Title Only](#) [Author and Title](#)

Henry A, Cal AJ, Batoto TC, Torres RO, Serraj R (2012) Root attributes affecting water uptake of rice (*Oryza sativa*) under drought. *J Exp Bot* 63: 4751–4763

Google Scholar: [Author Only](#) [Title Only](#) [Author and Title](#)

Hirsch CN, Foerster JM, Johnson JM, Sekhon RS, Muttoni G, Vaillancourt B, Peñagaricano F, Lindquist E, Pedraza MA, Barry K, et al (2014) Insights into the maize pan-genome and pan-transcriptome. *Plant Cell* 26: 121–135

Google Scholar: [Author Only](#) [Title Only](#) [Author and Title](#)

Hochholdinger F (2009) The Maize Root System: Morphology, Anatomy, and Genetics. *Handbook of Maize: Its Biology*. Springer New York, pp 145–160

Google Scholar: [Author Only](#) [Title Only](#) [Author and Title](#)

Ho MD, Rosas JC, Brown KM, Lynch JP (2005) Root architectural tradeoffs for water and phosphorus acquisition. *Funct Plant Biol* 32: 737–748

Google Scholar: [Author Only](#) [Title Only](#) [Author and Title](#)

Hose E, Steudle E, Hartung W (2000) Abscisic acid and hydraulic conductivity of maize roots: a study using cell- and root-pressure probes. *Planta* 211: 874–882

Google Scholar: [Author Only Title Only Author and Title](#)

Huang J, Kim CM, Xuan Y-H, Park SJ, Piao HL, Je BI, Liu J, Kim TH, Kim B-K, Han C-D (2013) OsSNBP1, a Sec14-nodulin domain-containing protein, plays a critical role in root hair elongation in rice. *Plant Mol Biol* 82: 39–50

Google Scholar: [Author Only Title Only Author and Title](#)

Huber W, Carey VJ, Gentleman R, Anders S, Carlson M, Carvalho BS, Bravo HC, Davis S, Gatto L, Girke T, et al (2015) Orchestrating high-throughput genomic analysis with Bioconductor. *Nat Methods* 12: 115–121

Google Scholar: [Author Only Title Only Author and Title](#)

Ingvarsson PK, Street NR (2011) Association genetics of complex traits in plants: Tansley review. *New Phytol* 189: 909–922

Google Scholar: [Author Only Title Only Author and Title](#)

IPCC (2013) *Climate Change 2013: The Physical Science Basis. Contribution of Working Group I to the Fifth Assessment Report of the Intergovernmental Panel on Climate Change*. Cambridge University Press

Google Scholar: [Author Only Title Only Author and Title](#)

Jaramillo RE, Nord EA, Chimungu JG, Brown KM, Lynch JP (2013) Root cortical burden influences drought tolerance in maize. *Ann Bot* 112: 429–437

Google Scholar: [Author Only Title Only Author and Title](#)

Jeong H, Mason SP, Barabási A-L, Oltvai ZN (2001) Lethality and centrality in protein networks. *Nature* 411: 41–42

Google Scholar: [Author Only Title Only Author and Title](#)

Jiao Y, Peluso P, Shi J, Liang T, Stitzer MC, Wang B, Campbell MS, Stein JC, Wei X, Chin C-S, et al (2017) Improved maize reference genome with single-molecule technologies. *Nature* 546: 524–527

Google Scholar: [Author Only Title Only Author and Title](#)

Johnsson C, Jin X, Xue W, Dubreuil C, Lezhneva L, Fischer U (2019) The plant hormone auxin directs timing of xylem development by inhibition of secondary cell wall deposition through repression of secondary wall NAC-domain transcription factors. *Physiol Plant* 165: 673–689

Google Scholar: [Author Only Title Only Author and Title](#)

Kadam NN, Tamilselvan A, Lawas LMF, Quinones C, Bahuguna RN, Thomson MJ, Dingkuhn M, Muthurajan R, Struik PC, Yin X, et al (2017) Genetic Control of Plasticity in Root Morphology and Anatomy of Rice in Response to Water Deficit. *Plant Physiol* 174: 2302–2315

Google Scholar: [Author Only Title Only Author and Title](#)

Kadam NN, Yin X, Bindraban PS, Struik PC, Jagadish KSV (2015) Does morphological and anatomical plasticity during the vegetative stage make wheat more tolerant of water deficit stress than rice? *Plant Physiol* 167: 1389–1401

Kaler AS, Purcell LC (2019) Estimation of a significance threshold for genome-wide associated studies. *BMC Genomics* 20: 1–8

Google Scholar: [Author Only Title Only Author and Title](#)

Kano M, Inukai Y, Kitano H, Yamauchi A (2011) Root plasticity as the key root trait for adaptation to various intensities of drought stress in rice. *Plant Soil* 342: 117–128

Google Scholar: [Author Only Title Only Author and Title](#)

Kariola T, Brader G, Helenius E, Li J, Heino P, Palva ET (2006) EARLY RESPONSIVE TO DEHYDRATION 15, a negative regulator of abscisic acid responses in Arabidopsis. *Plant Physiol* 142: 1559–1573

Google Scholar: [Author Only Title Only Author and Title](#)

Klein SP, Schneider HM, Perkins AC, Brown KM, Lynch JP (2020) Multiple Integrated Root Phenotypes Are Associated with Improved Drought Tolerance. *Plant Physiol* 183: 1011–1025

Google Scholar: [Author Only Title Only Author and Title](#)

Kolde R (2015) pheatmap: Pretty heatmaps.

Kruijer W (2019) heritability: Marker-Based Estimation of Heritability Using Individual Plant or Plot Data.

Kubo M, Udagawa M, Nishikubo N, Horiguchi G, Yamaguchi M, Ito J, Mimura T, Fukuda H, Demura T (2005) Transcription switches for protoxylem and metaxylem vessel formation. *Genes Dev* 19: 1855–1860

Google Scholar: [Author Only Title Only Author and Title](#)

Langfelder P, Horvath S (2008) WGCNA: an R package for weighted correlation network analysis. *BMC Bioinformatics* 9: 1–13

Google Scholar: [Author Only Title Only Author and Title](#)

Lewis AM, Boose ER (1995) Estimating Volume Flow Rates Through Xylem Conduits. *Am J Bot* 82: 1112–1116

Google Scholar: [Author Only Title Only Author and Title](#)

Liakat Ali M, Luetchens J, Nascimento J, Shaver TM, Kruger GR, Lorenz AJ (2015) Genetic variation in seminal and nodal root angle and their association with grain yield of maize under water-stressed field conditions. *Plant and Soil* 397: 213–225

Google Scholar: [Author Only Title Only Author and Title](#)

- Li H, Zhang D, Wang X, Li H, Rengel Z, Shen J (2018) Competition between Zea mays genotypes with different root morphological and physiological traits is dependent on phosphorus forms and supply patterns. *Plant Soil* 434: 125–137
Google Scholar: [Author Only](#) [Title Only](#) [Author and Title](#)
- Lipka AE, Tian F, Wang Q, Peiffer J, Li M, Bradbury PJ, Gore MA, Buckler ES, Zhang Z (2012) GAPIT: genome association and prediction integrated tool. *Bioinformatics* 28: 2397–2399
Google Scholar: [Author Only](#) [Title Only](#) [Author and Title](#)
- Lobell DB, Roberts MJ, Schlenker W, Braun N, Little BB, Rejesus RM, Hammer GL (2014) Greater sensitivity to drought accompanies maize yield increase in the U.S. Midwest. *Science* 344: 516–519
Google Scholar: [Author Only](#) [Title Only](#) [Author and Title](#)
- Lobell DB, Schlenker W, Costa-Roberts J (2011) Climate trends and global crop production since 1980. *Science* 333: 616–620
Google Scholar: [Author Only](#) [Title Only](#) [Author and Title](#)
- Lopes CT, Franz M, Kazi F, Donaldson SL, Morris Q, Bader GD (2010) Cytoscape Web: an interactive web-based network browser. *Bioinformatics* 26: 2347–2348
Google Scholar: [Author Only](#) [Title Only](#) [Author and Title](#)
- Lynch J, Epstein E, Lauchli A, Weight GI (1990) An automated greenhouse sand culture system suitable for studies of P nutrition. *Plant Cell Environ* 13: 547–554
Google Scholar: [Author Only](#) [Title Only](#) [Author and Title](#)
- Lynch JP (2013) Steep, cheap and deep: an ideotype to optimize water and N acquisition by maize root systems. *Ann Bot* 112: 347–357
Google Scholar: [Author Only](#) [Title Only](#) [Author and Title](#)
- Lynch JP (2019) Root phenotypes for improved nutrient capture: an underexploited opportunity for global agriculture. *New Phytol* 223: 548–564
Google Scholar: [Author Only](#) [Title Only](#) [Author and Title](#)
- Lynch JP (2018) Rightsizing root phenotypes for drought resistance. *J Exp Bot* 69: 3279–3292
Google Scholar: [Author Only](#) [Title Only](#) [Author and Title](#)
- Lynch JP, Chimungu JG, Brown KM (2014) Root anatomical phenes associated with water acquisition from drying soil: targets for crop improvement. *J Exp Bot* 65: 6155–6166
Google Scholar: [Author Only](#) [Title Only](#) [Author and Title](#)
- Mansueto L, Fuentes RR, Borja FN, Detras J, Abriol-Santos JM, Chebotarov D, Sanciangco M, Palis K, Copetti D, Poliakov A, et al (2017) Rice SNP-seek database update: new SNPs, indels, and queries. *Nucleic Acids Res* 45: D1075–D1081
Google Scholar: [Author Only](#) [Title Only](#) [Author and Title](#)
- Maurel C, Nacry P (2020) Root architecture and hydraulics converge for acclimation to changing water availability. *Nat Plants* 6: 744–749
Google Scholar: [Author Only](#) [Title Only](#) [Author and Title](#)
- Mazaheri M, Heckwolf M, Vaillancourt B, Gage JL, Burdo B, Heckwolf S, Barry K, Lipzen A, Ribeiro CB, Kono TJY, et al (2019) Genome-wide association analysis of stalk biomass and anatomical traits in maize. *BMC Plant Biology* 19: 1–17
Google Scholar: [Author Only](#) [Title Only](#) [Author and Title](#)
- McCouch SR, Wright MH, Tung C-W, Maron LG, McNally KL, Fitzgerald M, Singh N, DeClerck G, Agosto-Perez F, Korniliev P, et al (2016) Open access resources for genome-wide association mapping in rice. *Nat Commun* 7: 10532
Google Scholar: [Author Only](#) [Title Only](#) [Author and Title](#)
- McDermott JE, Taylor RC, Yoon H, Heffron F (2009) Bottlenecks and hubs in inferred networks are important for virulence in *Salmonella typhimurium*. *J Comput Biol* 16: 169–180
Google Scholar: [Author Only](#) [Title Only](#) [Author and Title](#)
- McLaren W, Gil L, Hunt SE, Riat HS, Ritchie GRS, Thormann A, Flicek P, Cunningham F (2016) The Ensembl Variant Effect Predictor. *Genome Biol* 17: 1–14
Google Scholar: [Author Only](#) [Title Only](#) [Author and Title](#)
- Milhinhos A, Miguel CM (2013) Hormone interactions in xylem development: a matter of signals. *Plant Cell Reports* 32: 867–883
Google Scholar: [Author Only](#) [Title Only](#) [Author and Title](#)
- Okekeogbu IO, Pattathil S, González Fernández-Niño SM, Aryal UK, Penning BW, Lao J, Heazlewood JL, Hahn MG, McCann MC, Carpita NC (2019) Glycome and Proteome Components of Golgi Membranes Are Common between Two Angiosperms with Distinct Cell-Wall Structures. *Plant Cell* 31: 1094–1112
Google Scholar: [Author Only](#) [Title Only](#) [Author and Title](#)
- Oyiga BC, Palczak J, Wojciechowski T, Lynch JP, Naz AA, Léon J, Ballvora A (2020) Genetic components of root architecture and anatomy adjustments to water-deficit stress in spring barley. *Plant Cell Environ* 43: 692–711
Google Scholar: [Author Only](#) [Title Only](#) [Author and Title](#)

Parent B, Hachez C, Redondo E, Simonneau T, Chaumont F, Tardieu F (2009) Drought and abscisic acid effects on aquaporin content translate into changes in hydraulic conductivity and leaf growth rate: a trans-scale approach. Plant Physiol 149: 2000–2012

Google Scholar: [Author Only](#) [Title Only](#) [Author and Title](#)

Pesquet E, Tuominen H (2011) Ethylene stimulates tracheary element differentiation in *Zinnia elegans* cell cultures. New Phytol 190: 138–149

Google Scholar: [Author Only](#) [Title Only](#) [Author and Title](#)

Pires MV, de Castro EM, de Freitas BSM, Souza Lira JM, Magalhães PC, Pereira MP (2020) Yield-related phenotypic traits of drought resistant maize genotypes. Environ Exp Bot 171: 1–10

Google Scholar: [Author Only](#) [Title Only](#) [Author and Title](#)

Portwood JL, Woodhouse MR, Cannon EK, Gardiner JM, Harper LC, Schaeffer ML, Walsh JR, Sen TZ, Cho KT, Schott DA, et al (2018) MaizeGDB 2018: the maize multi-genome genetics and genomics database. Nucleic Acids Research 47: 1146–1154

Google Scholar: [Author Only](#) [Title Only](#) [Author and Title](#)

Purushothaman R, Zaman-Allah M, Mallikarjuna N, Pannirselvam R, Krishnamurthy L, Gowda CLL (2013) Root Anatomical Traits and Their Possible Contribution to Drought Tolerance in Grain Legumes. Plant Prod Sci 16: 1–8

Google Scholar: [Author Only](#) [Title Only](#) [Author and Title](#)

Qin L-X, Li Y, Li D-D, Xu W-L, Zheng Y, Li X-B (2014) Arabidopsis drought-induced protein Di19-3 participates in plant response to drought and high salinity stresses. Plant Mol Biol 86: 609–625

Google Scholar: [Author Only](#) [Title Only](#) [Author and Title](#)

Ramachandran P, Augstein F, Nguyen V, Carlsbecker A (2020) Coping With Water Limitation: Hormones That Modify Plant Root Xylem Development. Front Plant Sci 11: 570

Google Scholar: [Author Only](#) [Title Only](#) [Author and Title](#)

Ramachandran P, Wang G, Augstein F, de Vries J, Carlsbecker A (2018) Continuous root xylem formation and vascular acclimation to water deficit involves endodermal ABA signalling via miR165. Development 145: 1-7

Google Scholar: [Author Only](#) [Title Only](#) [Author and Title](#)

R Core Team (2020) R: A language and environment for statistical computing. R Foundation for Statistical Computing, Vienna, Austria

Google Scholar: [Author Only](#) [Title Only](#) [Author and Title](#)

Richards RA, Passioura JB (1989) A breeding program to reduce the diameter of the major xylem vessel in the seminal roots of wheat and its effect on grain-yield in rain-fed environments. Aust J Agric Res 40: 943–950

Google Scholar: [Author Only](#) [Title Only](#) [Author and Title](#)

Richmond TA, Somerville CR (2000) The cellulose synthase superfamily. Plant Physiol 124: 495–498

Google Scholar: [Author Only](#) [Title Only](#) [Author and Title](#)

Roberts K, McCann MC (2000) Xylogenesis: the birth of a corpse. Curr Opin Plant Biol 3: 517–522

Google Scholar: [Author Only](#) [Title Only](#) [Author and Title](#)

Růžička K, Ursache R, Hejátko J, Helariutta Y (2015) Xylem development - from the cradle to the grave. New Phytol 207: 519–535

Google Scholar: [Author Only](#) [Title Only](#) [Author and Title](#)

Salse J, Piegue B, Cooke R, Delseny M (2004) New in silico insight into the synteny between rice (*Oryza sativa* L.) and maize (*Zea mays* L.) highlights reshuffling and identifies new duplications in the rice genome. The Plant Journal 38: 396–409

Google Scholar: [Author Only](#) [Title Only](#) [Author and Title](#)

Schaefer RJ, Michno J-M, Jeffers J, Hoekenga O, Dilkes B, Baxter I, Myers CL (2018) Integrating Coexpression Networks with GWAS to Prioritize Causal Genes in Maize. Plant Cell 30: 2922–2942

Google Scholar: [Author Only](#) [Title Only](#) [Author and Title](#)

Schaefer RJ, Michno J-M, Myers CL (2017) Unraveling gene function in agricultural species using gene co-expression networks. Biochim Biophys Acta Gene Regul Mech 1860: 53–63

Google Scholar: [Author Only](#) [Title Only](#) [Author and Title](#)

Schnable PS, Ware D, Fulton RS, Stein JC, Wei F, Pasternak S, Liang C, Zhang J, Fulton L, Graves TA, et al (2009) The B73 Maize Genome: Complexity, Diversity, and Dynamics. Science 326: 1112–1115

Google Scholar: [Author Only](#) [Title Only](#) [Author and Title](#)

Schneider HM, Klein SP, Hanlon MT, Kaeppler S, Brown KM, Lynch JP (2020a) Genetic control of root anatomical plasticity in maize. Plant Genome 13: 1–14

Google Scholar: [Author Only](#) [Title Only](#) [Author and Title](#)

Schneider HM, Klein SP, Hanlon MT, Nord EA, Kaeppler S, Brown KM, Warry A, Bhosale R, Lynch JP (2020b) Genetic Control of Root Architectural Plasticity in Maize. J Exp Bot 71: 3185–3197

Google Scholar: [Author Only](#) [Title Only](#) [Author and Title](#)

Schneider HM, Lynch JP (2020) Should Root Plasticity Be a Crop Breeding Target? Front Plant Sci 11: 1–16

Schuetz M, Smith R, Ellis B (2012) Xylem tissue specification, patterning, and differentiation mechanisms. J Exp Bot 64: 11–31

Google Scholar: [Author Only](#) [Title Only](#) [Author and Title](#)

Smith BG, Harris PJ (1999) The polysaccharide composition of Poales cell walls: Poaceae cell walls are not unique. Biochem Syst Ecol 27: 33–53

Google Scholar: [Author Only](#) [Title Only](#) [Author and Title](#)

Sosa JM, Huber DE, Welk B, Fraser HL (2014) Development and application of MIPARTM: a novel software package for two- and three-dimensional microstructural characterization. Integrating Materials and Manufacturing Innovation 3: 123–140

Google Scholar: [Author Only](#) [Title Only](#) [Author and Title](#)

de Souza TC, de Castro EM, César Magalhães P, De Oliveira Lino L, Trindade Alves E, de Albuquerque PEP (2013) Morphophysiology, morphoanatomy, and grain yield under field conditions for two maize hybrids with contrasting response to drought stress. Acta Physiol Plant 35: 3201–3211

Google Scholar: [Author Only](#) [Title Only](#) [Author and Title](#)

Sperry JS, Saliendra NZ (1994) Intra- and inter-plant variation in xylem cavitation in *Betula occidentalis*. Plant Cell Environ 17: 1233–1241

Google Scholar: [Author Only](#) [Title Only](#) [Author and Title](#)

Stelpflug SC, Sekhon RS, Vaillancourt B, Hirsch CN, Buell CR, de Leon N, Kaeppler SM (2016) An Expanded Maize Gene Expression Atlas based on RNA Sequencing and its Use to Explore Root Development. Plant Genome 9: 1–16

Google Scholar: [Author Only](#) [Title Only](#) [Author and Title](#)

Stöver BC, Müller KF (2010) TreeGraph 2: Combining and visualizing evidence from different phylogenetic analyses. BMC Bioinformatics 11: 1–9

Google Scholar: [Author Only](#) [Title Only](#) [Author and Title](#)

Strock CF, Schneider HM, Galindo-Castañeda T, Hall BT, Van Gansbeke B, Mather DE, Roth MG, Chilvers MI, Guo X, Brown K, et al (2019) Laser ablation tomography for visualization of root colonization by edaphic organisms. Journal of Experimental Botany 70: 5327–5342

Google Scholar: [Author Only](#) [Title Only](#) [Author and Title](#)

Szekerés M, Németh K, Koncz-Kálmán Z, Mathur J, Kauschmann A, Altmann T, Rédei GP, Nagy F, Schell J, Koncz C (1996) Brassinosteroids rescue the deficiency of CYP90, a cytochrome P450, controlling cell elongation and de-etiolation in *Arabidopsis*. Cell 85: 171–182

Google Scholar: [Author Only](#) [Title Only](#) [Author and Title](#)

Taylor NG, Howells RM, Huttly AK, Vickers K, Turner SR (2003) Interactions among three distinct CesA proteins essential for cellulose synthesis. Proc Natl Acad Sci U S A 100: 1450–1455

Google Scholar: [Author Only](#) [Title Only](#) [Author and Title](#)

Trachsel S, Kaeppler SM, Brown KM, Lynch JP (2010) Shovelomics: high throughput phenotyping of maize (*Zea mays* L.) root architecture in the field. Plant Soil 341: 75–87

Google Scholar: [Author Only](#) [Title Only](#) [Author and Title](#)

Turco GM, Rodriguez-Medina J, Siebert S, Han D, Valderrama-Gómez MÁ, Vahldick H, Shulze CN, Cole BJ, Juliano CE, Dickel DE, et al (2019) Molecular Mechanisms Driving Switch Behavior in Xylem Cell Differentiation. Cell Rep 28: 342–351.e4

Google Scholar: [Author Only](#) [Title Only](#) [Author and Title](#)

Uga Y, Sugimoto K, Ogawa S, Rane J, Ishitani M, Hara N, Kitomi Y, Inukai Y, Ono K, Kanno N, et al (2013) Control of root system architecture by DEEPER ROOTING 1 increases rice yield under drought conditions. Nat Genet 45: 1097–1102

Google Scholar: [Author Only](#) [Title Only](#) [Author and Title](#)

Vadez V (2014) Root hydraulics: The forgotten side of roots in drought adaptation. Field Crops Res 165: 15–24

Google Scholar: [Author Only](#) [Title Only](#) [Author and Title](#)

Vadez V, Kholova J, Medina S, Kakkera A, Anderberg H (2014) Transpiration efficiency: new insights into an old story. J Exp Bot 65: 6141–6153

Google Scholar: [Author Only](#) [Title Only](#) [Author and Title](#)

Vejchasarn P (2014) Nutritional and Genetic Architecture of Root Traits in Rice (*Oryza sativa*). Ph.D. The Pennsylvania State University.

Google Scholar: [Author Only](#) [Title Only](#) [Author and Title](#)

Vilagrosa A, Chirino E, Peguero-Pina JJ, Barigah TS, Cochard H, Gil-Pelegrín E (2012) Xylem Cavitation and Embolism in Plants Living in Water-Limited Ecosystems. In R Aroca, ed, Plant Responses to Drought. Springer-Verlag, pp 63–109

Google Scholar: [Author Only](#) [Title Only](#) [Author and Title](#)

Vogel J (2008) Unique aspects of the grass cell wall. Curr Opin Plant Biol 11: 301–307

Google Scholar: [Author Only](#) [Title Only](#) [Author and Title](#)

Wahl S, Ryser P (2000) Root tissue structure is linked to ecological strategies of grasses. New Phytol 148: 459–471

Google Scholar: [Author Only](#) [Title Only](#) [Author and Title](#)

Wang DR, Agosto-Pérez FJ, Chebotarov D, Shi Y, Marchini J, Fitzgerald M, McNally KL, Alexandrov N, McCouch SR (2018) An imputation platform to enhance integration of rice genetic resources. Nat Commun 9: 3519

Google Scholar: [Author Only](#) [Title Only](#) [Author and Title](#)

Wasson AP, Richards RA, Chatrath R, Misra SC, Prasad SVS, Rebetzke GJ, Kirkegaard JA, Christopher J, Watt M (2012) Traits and selection strategies to improve root systems and water uptake in water-limited wheat crops. J Exp Bot 63: 3485–3498

Google Scholar: [Author Only](#) [Title Only](#) [Author and Title](#)

Wickham H (2016) ggplot2: Elegant Graphics for Data Analysis. Springer-Verlag, New York

Google Scholar: [Author Only](#) [Title Only](#) [Author and Title](#)

Yamaguchi M, Goué N, Igarashi H, Ohtani M, Nakano Y, Mortimer JC, Nishikubo N, Kubo M, Katayama Y, Kakegawa K, et al (2010a) VASCULAR-RELATED NAC-DOMAIN6 and VASCULAR-RELATED NAC-DOMAIN7 effectively induce transdifferentiation into xylem vessel elements under control of an induction system. Plant Physiol 153: 906–914

Google Scholar: [Author Only](#) [Title Only](#) [Author and Title](#)

Yamaguchi M, Mitsuda N, Ohtani M, Ohme-Takagi M, Kato K, Demura T (2011) VASCULAR-RELATED NAC-DOMAIN 7 directly regulates the expression of a broad range of genes for xylem vessel formation: Direct target genes of VND7. Plant J 66: 579–590

Google Scholar: [Author Only](#) [Title Only](#) [Author and Title](#)

Yamaguchi M, Ohtani M, Mitsuda N, Kubo M, Ohme-Takagi M, Fukuda H, Demura T (2010b) VND-INTERACTING2, a NAC domain transcription factor, negatively regulates xylem vessel formation in Arabidopsis. Plant Cell 22: 1249–1263

Google Scholar: [Author Only](#) [Title Only](#) [Author and Title](#)

Yoshida S, Forno DA, Bhadrachalam A (1971) Zinc deficiency of the rice plant on calcareous and neutral soils in the philippines. Soil Sci Plant Nutr 17: 83–87

Google Scholar: [Author Only](#) [Title Only](#) [Author and Title](#)

Yu H, Greenbaum D, Xin Lu H, Zhu X, Gerstein M (2004) Genomic analysis of essentiality within protein networks. Trends Genet 20: 227–231

Google Scholar: [Author Only](#) [Title Only](#) [Author and Title](#)

Yu H, Kim PM, Sprecher E, Trifonov V, Gerstein M (2007) The importance of bottlenecks in protein networks: correlation with gene essentiality and expression dynamics. PLoS Comput Biol 3: e59

Google Scholar: [Author Only](#) [Title Only](#) [Author and Title](#)

Zaman-Allah M, Jenkinson DM, Vadez V (2011) A conservative pattern of water use, rather than deep or profuse rooting, is critical for the terminal drought tolerance of chickpea. J Exp Bot 62: 4239–4252

Google Scholar: [Author Only](#) [Title Only](#) [Author and Title](#)

Zhan A, Schneider H, Lynch JP (2015) Reduced Lateral Root Branching Density Improves Drought Tolerance in Maize. Plant Physiol 168: 1603–1615

Google Scholar: [Author Only](#) [Title Only](#) [Author and Title](#)

Zhang X, Pang J, Ma X, Zhang Z, He Y, Hirsch CN, Zhao J (2019) Multivariate analyses of root phenotype and dynamic transcriptome underscore valuable root traits and water-deficit responsive gene networks in maize. Plant Direct 3: 1–18

Google Scholar: [Author Only](#) [Title Only](#) [Author and Title](#)

Zhao K, Tung C-W, Eizenga GC, Wright MH, Ali ML, Price AH, Norton GJ, Islam MR, Reynolds A, Mezey J, et al (2011) Genome-wide association mapping reveals a rich genetic architecture of complex traits in Oryza sativa. Nat Commun 2: 467

Google Scholar: [Author Only](#) [Title Only](#) [Author and Title](#)

Zheng Z, Hey S, Jubery T, Liu H, Yang Y, Coffey L, Miao C, Sigmon B, Schnable JC, Hochholdinger F, et al (2020) Shared Genetic Control of Root System Architecture between Zea mays and Sorghum bicolor. Plant Physiol 182: 977–991

Google Scholar: [Author Only](#) [Title Only](#) [Author and Title](#)

Zhu J, Brown KM, Lynch JP (2010) Root cortical aerenchyma improves the drought tolerance of maize (Zea mays L.). Plant Cell Environ 9: 31

Google Scholar: [Author Only](#) [Title Only](#) [Author and Title](#)